LEPTON - HADRON SCATTERING

FROM SCALING VIOLATION TO HERA

Frank Sciulli
Columbia University

Contents:

© F. Sciulli 1992

I. Historical Context

A. Personal Memories of the Scaling Revolution

My assigned role, in this summer school celebrating the important discovery of scaling, is to summarize the period between the 1968 discovery and the present. As one who lived through that period as a postdoc and young faculty, I cannot resist starting with a personal perception of those exciting times.

In 1968, as a callow postdoc at Caltech, I was performing an experiment at Berkeley to test the semileptonic $\Delta S = \Delta Q$ rule, for which there had been some serious experimental questions. We were completing this experiment (which verified the validity of the rule) during the same period that Bob Wilson was providing Fermilab (known then as the "National Accelerator Laboratory") with a strong start. My colleagues and I began to think about several interesting experiments for the new laboratory.

Colleagues at Caltech had been involved in the earlier SLAC elastic scattering experiments, so there existed good and constant communication with events in northern California. The earliest information indicated that the cross-section for the inelastic processes was much larger than anticipated. No one quite knew what this meant, but most thought it must be important. Shortly after, when the data[1] were plotted with BJ's now famous x-variable[2], the phenomenal universality was obvious. It seemed to me at that point that everyone <u>knew</u> it was important, but <u>why</u> it was important was elusive. Feynman, I recall, was in a highly excited state about these data which he had personally seen on a trip north, and equally excited about the x-universality. His parton model had begun its development[3] at about that time; it was through him that I began to understand the implications of these data as signalling the point-like constituency of hadrons.

A year or so after the discovery, scaling had begun to be corroborated with data[4] from the bubble chamber neutrino experiment Gargamelle (GGM). The SLAC data were predominantly in the momentum transfer range $3 < Q^2 < 30\ \mathrm{GeV}^2$; the Gargamelle data were at even lower momentum transfers. One question which disturbed Feynman greatly was why this phenomenon should be apparent at such low Q^2. If hadrons of masses about a GeV had point-like constituents, scaling phenomena would be expected to become apparent at much higher energies. There was the very important question whether scaling might be a low Q^2 phenomenon that had nothing to do with the point-like hadronic structure. If, on the other hand, scaling were a consequence of point-like constituents, it should get even more universal and understandable at higher momentum transfers.

Another important problem of the time, dear to my heart, involved the nature of the weak interactions. It was clear from the well-verified selection rules that the weak interactions had a pleasing regularity, particularly when the process involved leptons. A critical question, difficult to explore directly, was the high energy behavior of weak interactions. When extrapolated to very high energies, the beautiful Fermi theory broke down -- giving cross-sections larger than the unitarity limit. Even the hypothesized W-boson did not remove this problem, though the limit was postponed to higher energy. The scaling discovery provided a picture wherein the high energy behavior of weak interactions could be experimentally explored with high rate neutrino-nucleon scattering.

If indeed there were point-like constituents of nucleons, neutrino interactions with nucleons would also be point-like; a neutrino experiment would provide interactions with center-of-mass energies much higher than previous investigations (though still considerably short of unitarity limits). In short, if quarks were real, the neutrino-quark interaction could be understood in detail and tests of the weak interaction could be carried to what was, at the time, a very high energy.

The late 1960's was the time to think about experiments for the new National Accelerator Laboratory. After a lot of thought, Barry Barish, Bill Ford and I at Caltech, together with Al Maschke from Fermilab, proposed an experiment using high energy neutrinos.[5] The proposal (E21) began for me more than two decades of commitment to the investigation of deep-inelastic scattering with neutrinos. In retrospect, I would specify as the two most important motivating experiments for me:
(a) the BNL neutrino experiment of 1964 that discovered the muon neutrino, demonstrating that one could make scientific measurements with neutrino beams; and,
(b) the SLAC deep-inelastic scattering experiment which discovered scaling.

This history of long involvement with neutrinos will, I hope, excuse the sometimes overuse of neutrino examples for illustration. Since the first scaling discovery, both neutrino and muon/electron beams have had major impact on the development of the field.

B. Quarks are Real!!!

"It is fun to speculate about the way quarks would behave if they were physical particles of finite mass (instead of mathematical entities as they would be in the limit of infinite mass)... A search for stable quarks would help to reassure us of the non-existence of real quarks."
M. Gell-Mann[6] - 1964

From an historical context, it cannot be overemphasized that the discovery of scaling changed in a fundamental way the picture we have of strongly interacting particles. Before scaling, strong interactions seemed a messy subject. One bright hope was the "Eightfold Way" of Gell-Mann; this approach had phenomenal success in describing the spectroscopy of hadrons and the magnetic moments of baryons. Although the picture, motivated by the mathematical group SU_3, had been highly successful in providing regularity to static hadronic properties, it said little about the dynamics of strong interactions. (It should be noted, however, that the sum rules of chapter V were first obtained with SU_3!) Indeed, the fact that physical quarks were not observable as isolated entities in the laboratory made it seem likely that the quark description was a nice tool but that is should not be taken too seriously, as illustrated by the above quote.

A decade after the spectacular 1964 advent of the Eightfold Way, these quarks appeared no longer to be a set of mathematical curiosities: quarks were particles -- as real as any, and more fundamental than most! Though stable quarks still existed only inside hadrons, few scientists doubted their reality. This revolution in our paradigm for hadronic matter was largely due to the discovery of scaling.

In the mid-1960's, hadronic matter seemed a kind of mushy, fluid-like material; ten years later, we were thinking of hadrons more like tiny atoms with hard cores (probably quarks). This intuitive picture was provided by experiment. The picture became even more tangible to experimentalists as it became clear that this paradigm of quarks, besides demonstrating beauty and simplicity, was also very useful! The utility of the concept is illustrated dramatically in figure I-1, where the measured jet cross-section is shown over several decades of cross-section and energy. The curves are calculated predictions and they are correct!

Physicists colliding hadrons with protons are able to calculate predictions to compare to observation, whether that observation be a known phenomenon or some postulated new phenomenon. The cross-

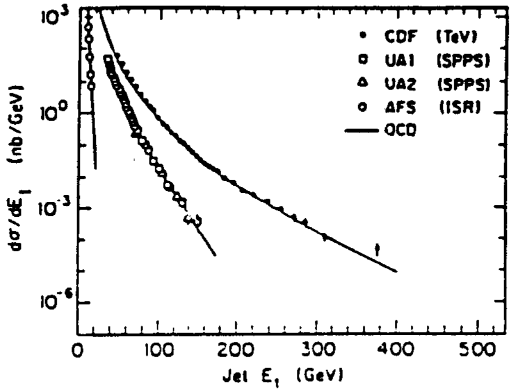

Figure I-1: Inclusive E_t spectrum from ISR, SPS, and Tevatron data. Curves are leading order QCD calculation. Normalizations are absolute.

section for the reaction of two hadrons, A and B, to create some specific final state, Γ,

$$A + B \to \Gamma + \text{hadronic debris}$$

may be calculated from a formula of the form:

$$E \frac{d^3\sigma}{dp^3} = \sum dx_A \, dx_B \, \rho_{i/A}(x_i,Q^2) \, \rho_{j/B}(x_j,Q^2) \, E_{ij} \frac{d^3\sigma(i+j\to\Gamma)}{d^3p_{ij}} . \qquad \text{(I-1)}$$

Here, Γ might be a J/ψ, a Z^0, or a pair of supersymmetric particles. Miraculously, probabilities for any hard hadronic process like these may be computed if the elementary cross-section, $\sigma(i + j \to \Gamma)$, on the far right-side of equation (I-1) is known from first principles, and if appropriate parton distributions (ρ) have been obtained from measurement. In the above equation, we need the probability, $\rho_{i/A}(x_i,Q^2)$, for finding a parton of type i, with momentum fraction, x_i, inside hadron A, as well as the probability for finding parton j inside B. These probabilities are simply derived from the structure functions divided by x, obtained as the principal consequence of deep-inelastic scattering experiments.

For the deep-inelastic scattering process of a neutrino (or antineutrino) with laboratory energy, E, incident on a fixed target nucleon of mass, M, contained in an isoscalar target (equal numbers of protons and neutrons):,

$$\nu_\mu(\bar{\nu})_\mu + N \to \mu^-(\mu^+) + X \qquad \text{(I-2)}$$

only a few parameters are needed to describe reactions. These include

(a) the square of the overall center-of-mass energy, $s = 2ME + M^2$, and

(b) the square of the momentum transfer, $Q^2 = -q^2$, between the lepton vertex and the hadron vertex.

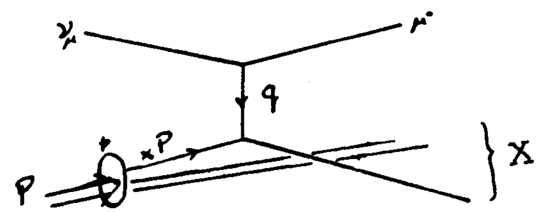

In addition, dimensionless scaling variables bring a pleasing simplicity to what would otherwise be very complicated. The first, $x = x_{BJ}$, has been described in detail in Sid Drell's lectures.[7] This parameter,

$$x = Q^2/2P\cdot q \quad \text{(I-3)}$$

is calculable for each event from measurable quantities of the event. Here P is the four-momentum of the target nucleon,

q is the four-momentum of the exchanged propagator, and

$Q^2 = -q^2$ is the invariant magnitude of this four-momentum.

If we consider a Lorentz frame in which the nucleon target is travelling at high momentum, x is the fraction of that momentum carried by the struck point-like parton. (See above sketch.)

The inelastisticity, or y-variable, is defined as

$$y = 2P\cdot q/(s - M^2) \; . \qquad \text{(I-4)}$$

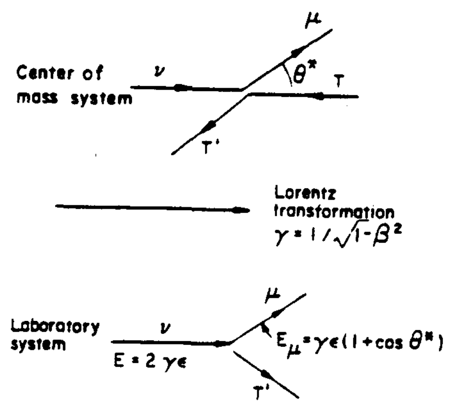

Figure I-2:

Lorentz transform from c.m. of point-like constituents to fixed-target laboratory.

All masses = 0;

All c. m. energies = ε.

$$1 - y = \frac{E_\mu}{E} = \frac{1 + \cos\theta^*}{2} \; ; \quad y = E_{T'}/E$$

In terms of fixed-target laboratory quantities, this is just the ratio of final state hadronic energy to incident neutrino energy, $y = E_h/E$. This has almost transparent significance in the limit of massless fermions as the scattering angle between the incident and outgoing lepton, θ^*, in the center-of-mass system between the incident neutrino and quark:

$$1 - y = (1 + \cos\theta^*)/2 \; . \qquad \text{(I-5)}$$

This is easily derived, as illustrated in figure I-2, by Lorentz transforming the incident and outgoing lepton energies from that system (where they are equal) and taking the ratio of laboratory energies. It follows that the distributions in y reflect directly the spin of the struck parton. Table I-1 shows the cases in neutrino and antineutrino scattering when striking spin 1/2 $(q,\bar{q})$ and spin 0 (k) partons. For any (V,A) interaction, it can be demonstrated that the scattering cross-section at high energy must be a linear combination of the three y-dependences shown.

Table I-1: y-dependence ($d\sigma/dy$) due to rotation matrix elements

Reaction	Ang Mom	Rotation Matrix	y-dependence
νq or $\overline{\nu q}$	0	1	1
$\nu\bar{q}$ or $\bar{\nu}q$	1	$\frac{1 + \cos\theta^*}{2}$	$(1-y)^2$
νk or $\bar{\nu}k$	1/2	$\cos(\theta^*/2)$	$(1-y)$

The formulae for very high energy neutrino and antineutrino scattering from an isoscalar target for the simplistic case where the partons are truly free and stationary are

$$\frac{d^2\sigma^{\nu N}}{dx\,dy} = \frac{G^2 s}{2\pi}\left[xq(x) + x\bar{q}(x)\,[1-y]^2 + 2\,xk(x)\,[1-y]\right]$$
$$\frac{d^2\sigma^{\bar{\nu} N}}{dx\,dy} = \frac{G^2 s}{2\pi}\left[x\bar{q}(x) + xq(x)\,[1-y]^2 + 2\,xk(x)\,[1-y]\right] \; . \qquad \text{(I-6)}$$

The function q(x) may be interpreted as the differential probability for finding a spin-1/2 point-like particle constituent with a fraction of the nucleon momentum between x and x+dx in a frame in which the nucleon is travelling relativistically. Similarly, $\bar{q}(x)$ is the distribution for pointlike antiparticle constituents, and k(x) is the distribution for non- spin 1/2 constituents.

The quark hypothesis for nucleon structure would imply, for $x > 0$, that

$$q(x) >> \bar{q}(x) >> k(x) . \qquad \text{(I-7)}$$

That is, the quark distributions should typically be larger than those for the antiquarks and both should dominate over the non-spin 1/2 components. In the "naive" parton model, the famous R-parameter (sometimes called the ratio of transverse to longitudinal cross-sections), given by

$$R = 2k(x)/[q(x)+\bar{q}(x)], \tag{I-8}$$

should be nearly zero. In the structure function language of the next section, this implies $F_2 = 2xF_1$, which goes under the name of the Callen-Gross relation.[8]

The structure functions (with R=0) are defined in terms of quark distributions as

$$\begin{aligned} F_2(x) &= xq(x) + x\bar{q}(x) \\ xF_3(x) &= xq(x) - x\bar{q}(x) \end{aligned} \tag{I-9}$$

The first is parity conserving; the second is parity-violating (and hence can only be observed through weak interaction processes). Of course, the hypothesis in this form is simplistic in that it neglects all the forces holding the quarks within the nucleon as well as the internal kinetic energies of those quarks. Such effects will contribute to a finite value for k(x) [or R]. Structure functions will also not truly be universal in x; that is, there will be some additional dependence on Q^2. We return to such effects in chapter IV.

The discovery of approximate scaling and the relatively small value of R at SLAC in the late 1960's clarified that, for electrons in the momentum-transfer range covered by SLAC, the quark hypothesis is valid. It was the job of experiments at higher energy over the ensuing years to corroborate this discovery, extend it to higher energies, and to make the tests more precise.

For neutrino interactions, the simplest expression of point-like constituents comes from simply integrating the expressions (I-6), in which the quantities in brackets integrate to constants. The resulting total cross-sections should rise linearly with laboratory neutrino energy, and the coefficients should be proportional to integrals over the functions q(x) and $\bar{q}(x)$. A glance at the expressions (I-6) and (I-7) indicates that the neutrino cross-section should be larger than that of the antineutrino. Indeed, the coefficients directly give the fraction of the nucleon momentum carried by quarks and antiquarks. This consistently has told us that the nucleon carries only about half its momentum in quarks and antiquarks, and that the antiquarks carry roughly twenty percent of this.

Figures I-3 gives a short summary of the history of total cross-section measurements. The earlier low energy Gargamelle data[9] indicated an approximately linear increase up to about E = 10 GeV: this is scaling behavior even though the cross-section in most of this range is dominated by the quasi-elastic process with a single nucleon in the final state. By 1975, it was clear that this qualitative behavior continues up to about 100 GeV, as shown in the top inset.[10] Five years later, the precision of experiments at FNAL and at CERN was such that the cross-section divided by energy, E, was typically plotted and precisions were approaching a few percent.[11]

There developed in the 1980's, however, an "East-West" effect: the values from Europe were lower than those in the US by about ten percent, as shown in the middle figure.[12] By 1985, these difficulties were clarified with the discovery of a calibration difficulty in the CERN narrow band flux system.[13] The bottom figure[14] shows that the cross-section measurements since then have been in good agreement, with linear slopes up to E =250 GeV. Next week, you will see newer data from the CCFR group[15] extending this range by about a factor of two.

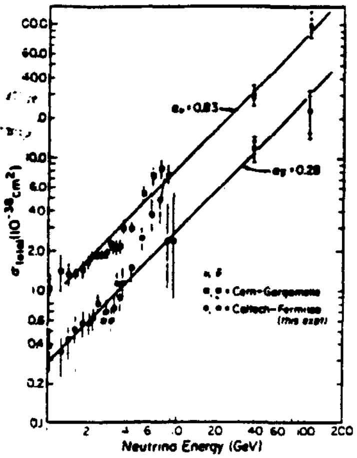

Figure I-3: History of ν, $\bar{\nu}$ total cross-section measurements. (See text.)
Top: 1975.
Middle: 1983.
Bottom: 1985.

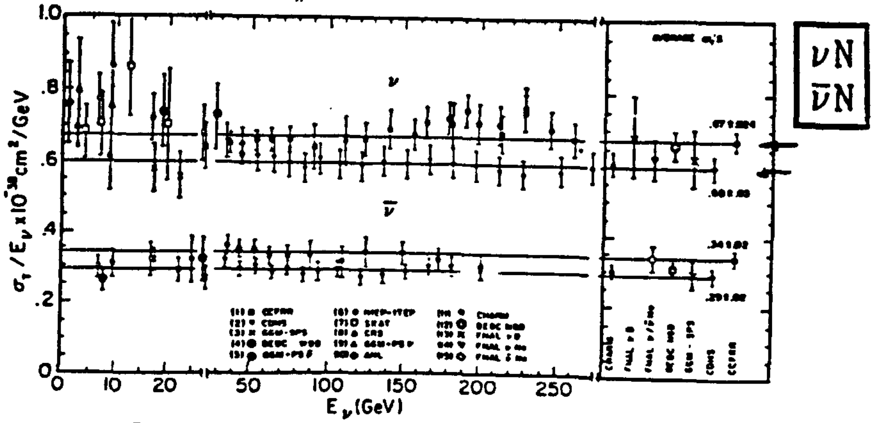

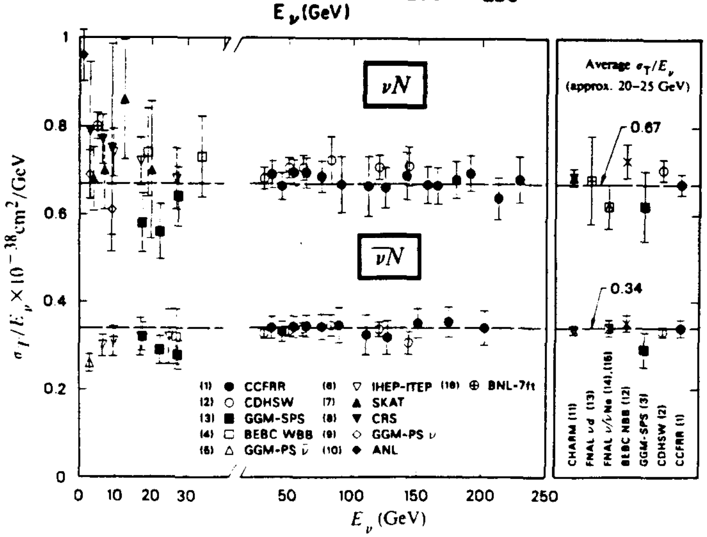

Demonstration of point-like constituents was the crux of the emerging picture. But a beautiful aspect of deep-inelastic scattering was the fact that the properties of these constituents could be directly measured. Already from the lower energy SLAC experiments, we knew that the struck constituents appeared to have spin 1/2 --- the demonstration of R << 1. In the mid 1970's, one neutrino experiment indicated some problem[16] with the simple quark picture, based on what appeared as anomalies in the y-distributions for antineutrinos at high energies. The interpretation was thought to show "effective violations of both scale invariance and charge-symmetry invariance."

But, over the next few years, several high energy experiments had shown that the y-dependence of the neutrino cross-sections had the form expected on the basis of the quark model.[17] A typical example of the experimental y-dependence is shown in figure I-4, where the quark and antiquark components in neutrino and antineutrino y-distributions are clearly seen.[18] Today, data up to energies of order 500 GeV show dependences on all the kinematic variables which are qualitatively consistent with the quark-parton model and quantitatively consistent with QCD.[19]

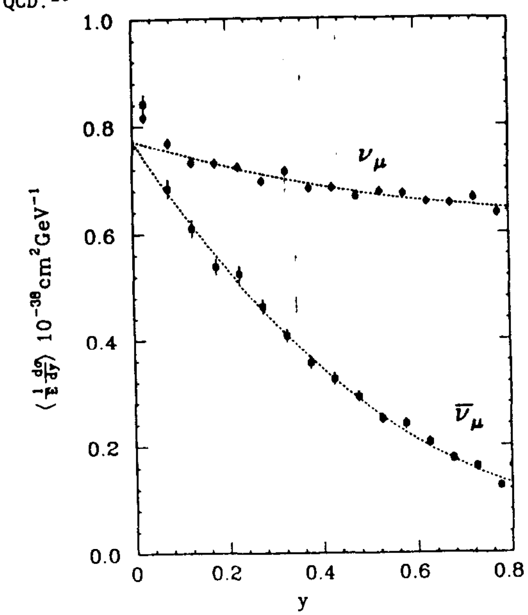

Figure I-4: CCFR data showing q and $\bar{q}$ contributions to ν and $\bar{\nu}$ y-distributions.

A third critical test of the quark model is the measurement of constituent charge. Because neutrinos couple to quarks through weak bosons, the integrated structure functions from $(\nu_\mu, \bar{\nu}_\mu)$ essentially count the <u>number</u> of quarks; electron and muon scattering experiments, because they couple with photons, determine integrated structure functions which depend on the sum of the mean square electric charges from all scattered constituents. The ratio of structure functions from the two techniques is therefore proportional to the mean square of constituent charge. This test is non-trivial: for fractionally charged quarks the ratio should be 5/18, whereas if integral charges were involved, we expect a value typically between 1/2 and unity.

Figure I-5: Test of constituent nucleon charges (see text).

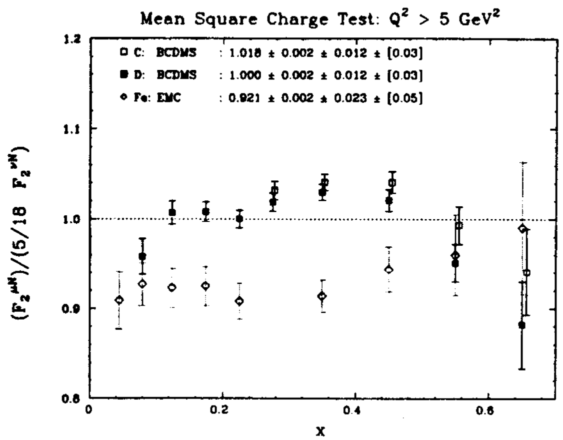

Figure I-5 shows recent results on this ratio (as a function of x) for structure functions from the CCFR neutrino experiment normalizing various high energy muon structure functions. The seven percent adjustment on the EMC data is now rather generally agreed to be necessary.[20] Note the suppressed scale, and the integral-charged quarks would likely produce a value between 1.8 and 3.6 on this scale. The data clearly show that the constituents have the charges expected for quarks.

C. Cross-section Formulae for Deep Inelastic Scattering

For completeness, we provide here the formulae for inelastic scattering appropriate to neutrino scattering from an isoscalar nucleon (i.e., the average for neutrons and protons):

$$\frac{d^2\sigma^{\nu N}}{dx\,dy} = \frac{G^2 M\ E}{\pi}\left[F_2^{\nu N}(x,Q^2)[1-y+Mxy/2E] + 2xF_1^{\nu N}(x,Q^2)[y^2/2] + xF_3^{\nu N}(x,Q^2)\ y[1-y/2]\right] . \quad \text{(I-10)}$$

For antineutrino scattering from an isoscalar nucleon, the expression is identical except the last term (xF_3) enters with opposite sign. The analogous expression for muon or electron scattering from isoscalar nucleons may be obtained by making the formal replacements in reaction (I-10):

$$\begin{aligned} &G^2/\pi \rightarrow 8\pi\alpha^2/Q^4; \\ &F_2^{\nu N}(x,Q^2) \rightarrow F_2^{\mu N}(x,Q^2); \\ &xF_1^{\nu N}(x,Q^2) \rightarrow xF_1^{\mu N}(x,Q^2); \\ &xF_3^{\nu N}(x,Q^2) \rightarrow 0. \end{aligned} \quad \text{(I-11)}$$

The function, xF_3, does not contribute since the muon scattering reaction at fixed target energies is parity-conserving.

The relationship between the structure functions, F_2 and $2xF_1$, provides the definition for R:

$$\frac{2xF_1}{F_2} = \frac{1 + 4M^2x^2/Q^2}{1 + R} . \quad \text{(I-10)}$$

II. A New Weak Current

The advent of deep inelastic scattering, and its demonstration of the quark constituency of hadrons, ushered in several decades of research using the new technique of deep inelastic scattering for understanding details of hadronic structure and hadronic forces. But time soon demonstrated it as a tool for investigating the nature of weak interactions as well. It was through deep inelastic scattering that the neutral weak current was originally found and it was largely using deep inelastic scattering that the predicted properties of the neutral current were verified.

In 1968, the very beautiful electroweak unification of SU_2xU_1 was predicted by Weinberg and Salam.[21] The experimental search for the consequences of this prediction had an interesting history.[22] At the time of the prediction, there were very strong limits on the absence of strangeness-violating decays ($\sim 10^{-7}$) relative to the ordinary charged-current processes. But strangeness- (or flavor-) conserving processes were much more difficult to investigate, since such decays would be swamped by strong or electromagnetic decays. The only practical way to find them directly was through neutrino interactions. That is, the new process

$$\nu_\mu(\bar{\nu}_\mu) + N \rightarrow \nu_\mu(\bar{\nu}_\mu) + X \qquad \text{(II-1)}$$

should accompany the analogous "ordinary" deep-inelastic processes (I-2). At the time under discussion, the best limits on such reactions would come from neutrino experiments by the Gargamelle bubble chamber group at the 30 GeV CERN PS. Experimental detection of "muonless" events was complicated by the possibility of neutron-induced background from the relatively dense material surrounding the bubble chamber. Understanding the background to the necessary level was not easy. Frankly, though, in 1968 the prediction of neutral currents did not get much experimental attention.

In 1971, it was demonstrated that the SU_2xU_1 theory was but one example of a gauge theory which was in principle renormalizable to all orders of perturbation theory.[23] This created a heightened interest in SU_2xU_1, as well as a surge of interest in other gauge theories, some with very different predictions.[24] At the 1972 international conference held at Fermilab, there were limits (some lower than predicted by SU_2xU_1) placed on many exclusive neutrino-induced neutral current processes, as well as on the deep-inelastic process.[25]

The first reported observation of flavor-conserving neutral currents came from the Gargamelle group in 1973.[26] This group began to see evidence for the inelastic process II-1,[27] as well as one example of the purely leptonic elastic scattering of antineutino by electron.[28] Since the same group had previously quoted rather stringent bounds on the inelastic process,[29] and these bounds were limited by the presence of neutron-induced backgrounds, there was skepticism. Early searches at the new Fermilab accelerator by the HPWF group in 1973 and 1974, although corroborative of the existence of such processes, were not consistent with the rates predicted in SU_2xU_1.[30]

By the time of the next international conference in London in 1974, there began to be corroboration for the existence of neutral current processes.[31] The Gargamelle group now had two candidate events for the elastic scattering of electrons by muon neutrinos,[32] and several experiments saw exclusive channels at the two standard deviation level. Two experiments had very strong evidence for neutrino induced processes without neutron background. One (at BNL) measured the neutron background using time-of-flight.[33]

A significant corroboration of the existence of reaction (II-1) utilized the new "narrow band neutrino beam" at Fermilab.[34] The experiment cleanly demonstrated the existence of reactions induced by muon-type neutrinos, but with no muon in the final state. The spectrum of observed hadronic energies and the very large, dense target were such that it was clear that the reactions were initiated by neutrinos and that energy was transported out of the iron target by a weakly interacting neutral particle in the final state. Furthermore, the frequency of these interactions was consistent with the predictions of the Weinberg-Salam theory.

Over the next five years, there were many measurements of the rates for the neutral current inelastic reactions, as well as further observations of neutrino-electron scattering induced by neutral currents. Interest surged to verify in as many ways as possible that we indeed were seeing SU_2xU_1. Neutrino experiments proceeded to measure the rates for the new processes, and indeed found them to be consistent with the SU_2xU_1 picture.

Left directly untested were certain characteristics of the new interaction, like the spin of the exchanged boson. Such information could be obtained from processes in which the parity-violating weak process interferes with the well-known electromagnetic interaction. Zel'dovich had suggested much earlier that interference effects could be visible from parity-violating processes by means of very precise experiments. One involved laser light: a small rotation of the polarization plane by scattering from atoms. By 1977, limits had been placed on this effect and these limits were about a factor three smaller than the Weinberg-Salam prediction. (The following year, a finite effect was observed, and over the next several years, with improvements in understanding of atomic wavefunctions and in experimental techniques, theory and experiment converged to agreement.)

Another suggestion by Zel'dovich was to look for small parity violations using polarized electrons scattered from nucleons. In 1978, parity violation in the deep-inelastic process

$$e + p \rightarrow e + X \qquad \text{(II-2)}$$

was observed at SLAC. The effect is a small one, of order M_Z^2/Q^2, or $\sim 10^{-4}$. The experimenters were able to see asymmetry as a function of the polarization of the incident electron by using the g-2 precession of the electron in the beam transport system and measuring the asymmetry as a function of beam energy. Figure II-1 shows this result. The measurement was consistent with the Weinberg-Salam prediction, and demonstrated clearly that the small diagram with a new exchanged boson in the new neutral current process interferes with the dominant diagram involving photon exchange.

Today, there are many measurements of the neutral current parameters, as well as measured properties for the charged and neutral bosons.[35] But the history of the subject was one in which deep-inelastic scattering played a crucial role.

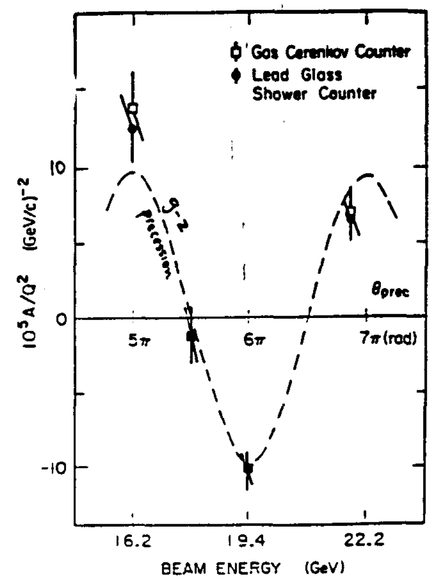

Figure II-1: Observed asymmetry versus laboratory beam energy. The variation is due to the precession in the transport bending magnet:

$\theta_{prec} = \gamma\, \theta_{bend}\, (g-2)/2$

$= \pi\, E_{beam}/3.237$ (GeV)

III. Parton Densities

The structure functions described in the last lecture originate as the densities of the several quark flavors inhabiting the nucleon. The broad experimentally observed features of structure functions argue strongly for this interpretation: rapidly varying dependence on x and gentle or logarithmic dependence on Q^2 at fixed x. This small dependence on Q^2, now understood as required by QCD, will be largely ignored in this discussion. We will return to the dependence on Q^2 in chapter IV.

Over the regime of energy and momentum transfers explored to date, we have measured the nucleon's composition in terms of u, d, and s quark densities. (The effects of higher mass quark constituents is generally ignored; this is likely a good approximation.) From the integral of the F_2 structure function, we know that half the nucleon momentum is carried by gluons. The gluon differential density cannot be directly measured in deep inelastic scattering because gluons carry no weak or electric charge, and hence are not scattered. However, there are methods for indirectly measuring gluons which also will be discussed in chapter IV. New methods are being developed for measuring the gluons, primarily applicable at HERA energies. These will be discussed in detail by Feltesse in his lectures at this school.

The <u>number</u> of u-quarks in the proton between x and x+dx is $u_p(x)dx$. [The proton is conventionally implied unless otherwise stated; that is, $u(x) = u_p(x)$.] Requirements of charge symmetry, or isospin, imply for example that the density of down quarks in the neutron should equal the density of up quarks in the proton. Specifically,

$$u(x) = u_p(x) = d_n(x) \qquad d(x) = d_p(x) = u_n(x)$$
$$\bar{u}(x) = \bar{u}_p(x) = \bar{d}_n(x) \qquad \bar{d}(x) = \bar{d}_p(x) = \bar{u}_n(x). \tag{III-1}$$

Note that integrals over these densities give the <u>total</u> numbers of quarks of each type. For example, integrating over the entire range $0 < x < 1$,

$$\int[u(x) - \bar{u}(x)]dx = \text{net number of u-quarks in the proton.}$$

Such relations reassure us that all quantum numbers are as defined for the proton and neutron. We return to this important topic later in our discussion of sum rules.

In chapter I, we discussed the quark (q) and anti-quark ($\bar{q}$) densities. Measured on isoscalar targets, these are given in terms of flavored quark densities as

$$q(x) = u(x) + d(x) + s(x) + c(x)$$
$$\bar{q}(x) = \bar{u}(x) + \bar{d}(x) + \bar{s}(x) + \bar{c}(x). \tag{III-2}$$

At fixed target energies, it is generally assumed that the charm constituency is negligible $[c(x) = 0]$.

A. Valence and Sea Quark Densities from Isoscalar Targets

There will be occasion to refer to "valence quark" and "sea (or ocean) quark" densities. These are respectively the quark densities defining the quantum numbers of the nucleon and the sea of quark and antiquark pairs. They are defined as

$$q_V(x) = q(x) - \bar{q}(x)$$
$$q_S(x) = \bar{q}(x)\ . \tag{III-3}$$

The valence and sea densities are relatively well-measured because they can be obtained from experiments using heavy nuclear targets.

The valence (essentially the xF_3 structure function from isoscalar targets) and sea distributions from recent CCFR data[36] are contrasted in figure III-1. (Note the logarithmic scales on these figures.) The valence distribution rises from zero at x=0, peaks at about 0.2 and falls roughly like a power of (1-x). The sea distribution, in contrast, is finite at x=0 and falls much faster with x.

B. u- and d-quark Densities

We outline here how individual quark densities are measured. For pedagogical reasons, only u and d quarks are considered. (The strange, or s-quarks, can be measured directly also; this will be discussed later.) The most unambiguous technique for separating the individual u- and d-quark and antiquark densities is to measure them with neutrinos and antineutrinos impinging on hydrogen and deuterium targets. For the scattering of neutrinos and antineutrinos from protons and neutrons, the cross-sections are proportional to

$$\begin{aligned}
\nu p:&\quad xd(x) + x\bar{u}(x)(1-y)^2\\
\nu n:&\quad xu(x) + x\bar{d}(x)(1-y)^2\\
\bar{\nu} p:&\quad xu(x)(1-y)^2 + x\bar{d}(x)\\
\bar{\nu} n:&\quad xd(x)(1-y)^2 + x\bar{u}(x).
\end{aligned}\qquad\text{(III-4)}$$

Measurements provide four separate data points and four unknowns at each value of x. Unfortunately, it is very difficult to obtain adequate numbers of events to make this separation with data from the light nucleon targets.

Higher statistical precision from hydrogen and deuterium targets is available with electron or muon beams. The cross-sections for scattering of charged leptons from protons or neutrons have the following y-dependence:

FIGURE III-1

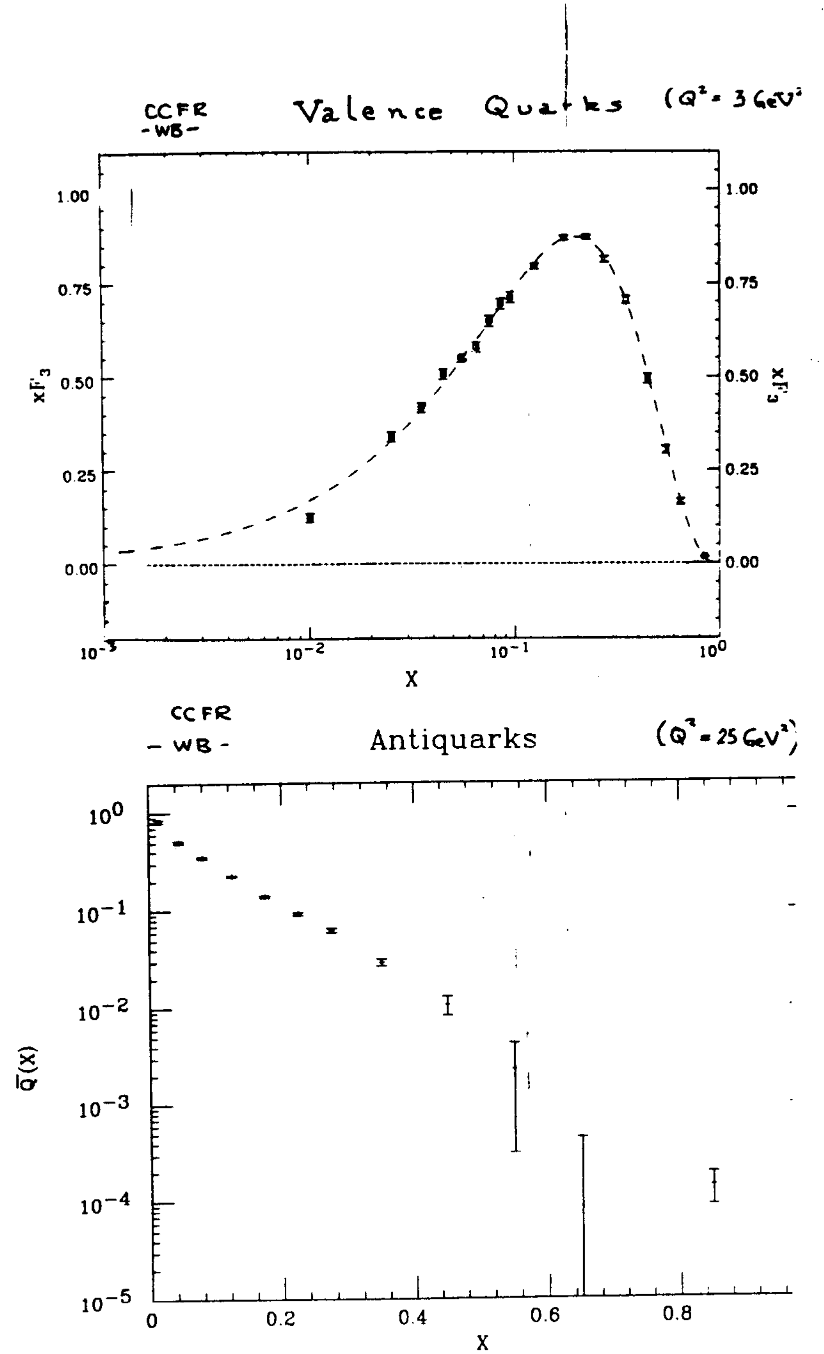

μ(or e)p: $\quad x[(d+\bar{d}) + 4(u+\bar{u})][1+(1-y)^2]/9$ (III-5)

μ(or e)n: $\quad x[(u+\bar{u}) + 4(d+\bar{d})][1+(1-y)^2]/9.$

A consequence of the vector nature and the charge coupling of the electromagnetic current is the appearance of the combination (particle + antiparticle) in both equations. Separation of a flavored quark from its antiquark requires additional assumptions about the nature of the sea and the valence constituencies; these are obtained from neutrino experiments.

Note that the ratio of F_2 obtained in e,μ experiments from neutron and proton targets is independent of y:

$$\frac{F_2^{en}}{F_2^{ep}} = \frac{1 + 4(d+\bar{d})/(u+\bar{u})}{4 + (d+\bar{d})/(u+\bar{u})} . \qquad \text{(III-6)}$$

Figure III-2 shows the behavior of F_2^{en}/F_2^{ep} from recent and older data.[37] As x gets large, the ratio approaches 1/4. Since valence quarks dominate at large x, it follows that the u-quark density becomes much larger than the d-quark density:

$$d/u \to 0 \text{ as } x \to 1.$$

Another interesting feature of this ratio is the behavior as $x \to 0$. Here we expect that $u(0) \to \bar{u}(0)$ [similarly $d(0) \to \bar{d}(0)$] so that the above ratio should approach unity. Indeed, if this were <u>not</u> true, certain sum rules (to be discussed) would have serious difficulty, not just to conform to prediction, but even to converge to a *finite result: the entire quark-parton picture would have serious* problems. The data of figure III-2 agree well with the hypothesized approach to unity at small x.

FIGURE III-2

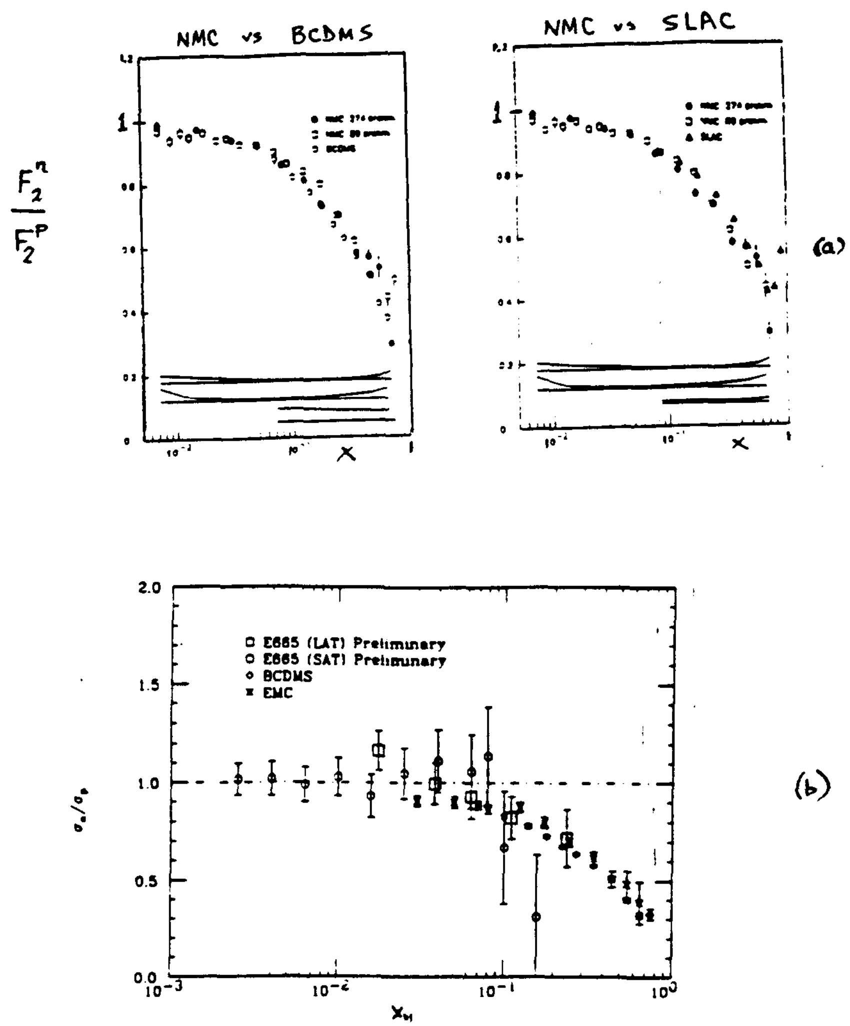

The individual flavor components of the valence and sea quark distributions are not well measured. A compilation of u- and d-valence quark distributions from last year[38] is shown in figure III-3 from several neutrino experiments and from the EMC muon experiment. Also shown as smooth curves are parametrizations[39] from data available at that time. The data generally have poor precision. The muon scattering data are systematically different for the valence d-quark distribution. New information from the muon experiments, and a recent re-evaluation of the overall normalization for the EMC structure functions,[40] may well bring these into better agreement. For the separate flavor components of antiquarks, the precision is even worse. Some information on this question comes from the Gottfried Sum Rule, discussed in chapter V.

Figure III-3: Separated flavors of valence components for the proton.

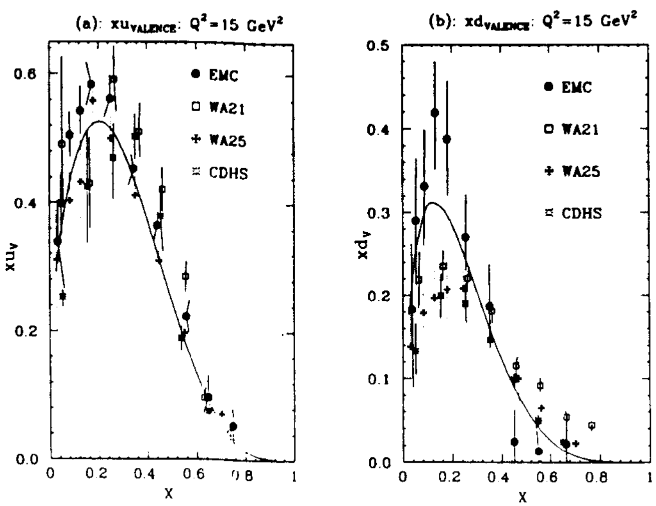

C. The Strange Quark Density

Neutrinos produce single charmed (c-) quarks from both s- and d-quarks; the resulting charmed mesons sometimes decay with a muon in the final state. These facts imply that roughly one percent of neutrino interactions contain two final state muons; such muons are easily detected with the large neutrino detectors in which a few millions of events, and of order ten thousand dimuon events are collected. The elementary processes creating these muons are

$$\nu_\mu + (d,s) \rightarrow \mu^- + c + X \qquad \text{(III-7)}$$
$$\bar{\nu}_\mu + (\bar{d},\bar{s}) \rightarrow \mu^+ + \bar{c} + X \ .$$

Here the charm quark, created with a μ^-, emerges as a charmed particle (typically D^0 or D^+) which subsequently decays, e.g., $D^0 \rightarrow \mu^+ + X$. The anticharm quark (created with a μ^+) can decay only to μ^-. In general, the processes (III-7) must lead to two final state muons of opposite sign.

The $d(\bar{d}) \rightarrow c(\bar{c})$ conversions in the above reactions are Cabibbo suppressed, whereas production from strange quarks is Cabbibo-favored. Hence, almost all dimuons created by antineutrinos are made from strange quarks, while only about half those created by neutrinos are from strange quarks.

Modelling these production processes is straightforward, though somewhat complicated by the threshold behavior for production of charmed particles at present fixed target energies. The charm threshold is typically described using the "slow-rescaling" formulation,[41] parametrized by an effective charm quark mass, m_c. The magnitude of the strange quark component is specified with the single parameter

$$\kappa = 2s/(\bar{u} + \bar{d}) \ . \qquad \text{(III-8)}$$

The constant multiplying the charged-current weak coupling between d- and c-quarks is the element, V_{cd}, of the Kobayashi-Moskawa matrix. For this process, it always occurs in the combination, $B|V_{cd}|^2$, where B is the branching fraction for D-mesons to decay into a charged muon. The results from three experiments[42] are shown in table III-1.[43]

Table III-1: κ and B from neutrino induced $\mu^+\mu^-$ events

Group	κ	$\lvert V_{cd}\rvert$	m_c (GeV)
CDHSW	0.474±.082±.046	.188 ± .018	
FMM	0.528±.200±.122		
CCFR	0.502±.078±.029	.213 ± .014	$1.34 \pm .24^{+.25}_{-.04}$
Avg	0.492±.054±.024	.204 ± .012	

Figure III-4 shows, from the CCFR experiment, the x-distribution for the strange and antistrange sea compared with the antiquark distribution. There is an indication that the strange sea distribution may be more steeply falling than that of the antiquark average.[44]

Figure III-4: Strange quark momentum distributions xs(x) and $x\bar{s}(x)$ compared with the $x\bar{q}(x)$ distribution. The smooth curve is a fit to the latter.

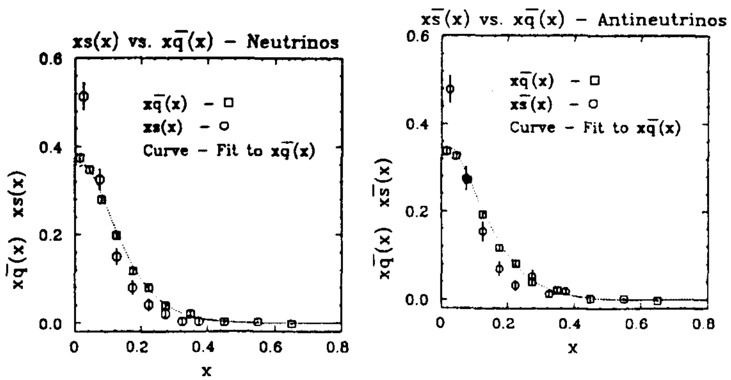

D. Global Fits to Parton Distributions

There are many groups which have assumed the nontrivial task of incorporating all deep inelastic data, as well as other relevant measurements, in order to obtain global parametrizations to the individual parton densities.

Figure III-5 shows a few examples[45] of these parametrizations. In essentially all cases, the fits have been evolved according to the requirements of QCD to much higher Q^2 to provide predictions for collider processes. While these global fits are good working hypotheses, the user should be aware of some of the limitations and disagreements among data which enter these parametrizations. For example, the use of EMC versus BCDMS data gives somewhat differing results, as seen by the left(EMC) and right(BCDMS) parts of the upper figure. Extrapolations to $Q^2 = M_W^2$ give differing predictions as well as seen in the lower figure.

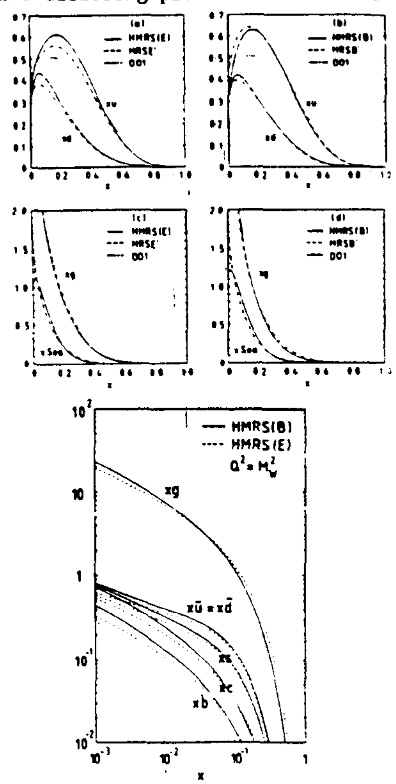

Figures III-5: Examples of parametizations of structure function data. Upper figures correspond to various fits to data at $Q^2 = 20\ \text{GeV}^2$. Lower curve (with logarithmic scale) are the extrapolated structure functions at $Q^2 = M_W^2$.

E. Effect of Nuclear Environment on Parton Densities

It has been known for some time that structure functions measured on free nucleons are not identical to those obtained from nucleons bound in heavy nuclei. Figure III-6 illustrates the x-dependence of this phenomenon, as obtained from several measurements of electron or muon scattering. There are three regions in x that can be delineated.

At large values ($x > .6$), we expect the effects of the Fermi motion of the nucleons to make a substantive effect. Consider the definition of x in terms of Lorentz invariants, $x = Q^2/2P\cdot q$. The numerator, as determined from the initial and final state leptons, will be unaffected by the nucleon binding. The denominator, on the other hand, cannot be so simply obtained; that is, $P\cdot q \neq M\nu$, where ν

Figure III-6: The EMC effect illustrating dependence of $F_2(A)/F_2(D)$ as a function of x.

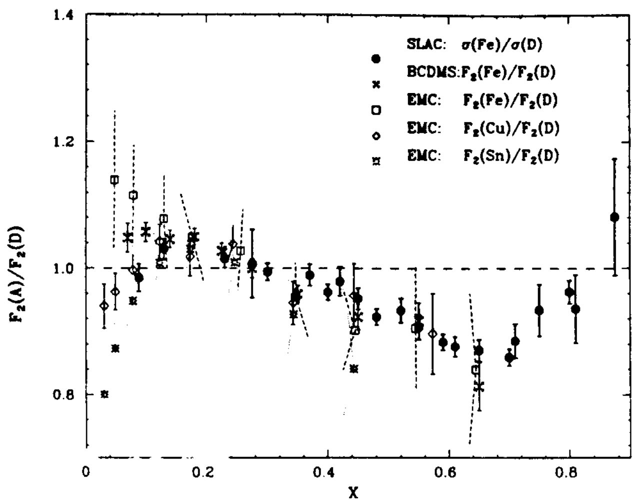

is the energy transferred to the hadron system (E_H). Instead, for a bound nucleon

$$P\cdot q = M\nu - p_z|\vec{q}| \qquad \text{(III-9)}$$

where

$|\vec{q}|$ is the magnitude of the spacelike momentum transfer and

p_z is the component of the nucleon Fermi momentum in the spatial direction of $\vec{q}$. Hence, if we specify the <u>measured</u> momentum fraction as $x_m = Q^2/2M\nu$, then the actual momentum fraction for the struck quark is

$$x = x_m/(1 + p_z/M) \qquad \text{(III-10)}$$

at large Q^2. (Terms of order Q^2/ν^2 have been ignored.) Since p_z is not known for an individual event, the x-distribution as measured from bound nucleons will be the free nucleon distribution smeared over the distribution in Fermi momentum with the factor $(1 + p_z/M)$: this moves x randomly by about 20% of x. This effect is largely independent of Q^2. It will also typically be a small effect except at large x, where the free nucleon structure functions must approach zero (from momentum conservation) but the bound nucleon structure functions are finite. The rise in the ratio shown in figure III-6 at large x is primarily due to this effect. (Note that the sumrules and QCD tests should be independent of whether the nucleon is bound or not.)

At very small x, nucleons are shadowed by the others bound in a heavy nucleus.[46] This phenomenon has been known for some time in the scattering of real photons by nuclei. As $Q^2 \to 0$, virtual photons must approach the behavior of real photons. Figure III-7 shows the ratio at very small x for Xe and D_2 as targets, from two recent experiments which verify this effect.[47] Hence, the behavior for $x \leq 0.1$ in figure III-6 is largely due to shadowing. There is considerable theoretical activity in attempting a quantitative explanation for this shielding effect.[48] Such explanations lead us to expect little Q^2 dependence in this region also, which is consistent with recent measurements.[49]

Figure III-7: Xe to D_2 cross-section ratio at small x.

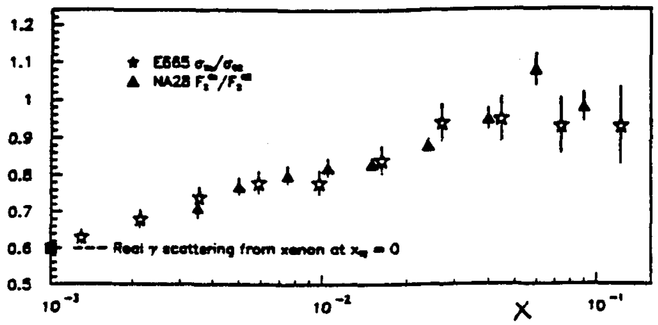

The intermediate region, 0.1 < x < 0.6, also shows clear differences between heavy and light nuclei in figure III-6. This was a surprise when first seen nearly ten years ago[50] and was dubbed the "EMC effect." While the effect is clearly established,[51] and it is known that there is little dependence (at fixed x) on Q^2, there are several theoretical conjectures for its origin. These range from assertions that the effective momentum transfer in heavy nuclei is different from that in a free nucleon, to effects on the antiquark component due to the existence of additional virtual mesons in a large nucleus. The reader is referred to a recent review of this interesting question.[52]

F. Non-spin 1/2 Parton Density (R)

Scattering from a non-spin 1/2 component of the nucleon, denoted k(x) in chapter I, should give a measurable y-dependence. This is parametrized by R as defined in equations (I-8) and (I-12). The very earliest discovery experiments[1] at SLAC recognized that this parameter was small ($R \leq 0.2$), in qualitative agreement with the constituent quark model. A small value of R could easily be accommodated in the pre-QCD quark model; the origin is due to effects of the quark binding within the nucleon. Such binding would entail finite transverse momentum (k_t) of the quarks leading to a collision with the lepton which is non-colinear in any frame obtained by a Lorentz transformation along the beam direction. These effects must create a finite value[53] of R:

$$R = 4\langle k_t^2\rangle/Q^2 \qquad \text{(III-11)}$$

which should decrease quickly with Q^2. (We shall deal in the next chapter with a different prediction from QCD which predicts a finite value of R depending logarithmically on Q^2.)

The early SLAC experiments were not precise enough to determine whether R was falling with x and Q^2. Later measurements showed that the value was even smaller than 0.2 at larger values of Q^2. These different data have been nicely tied together by a recent SLAC experiment,[54] which clearly delineates that R falls with Q^2 and with x. We will return to this topic in the next section.

IV. QCD in Deep Inelastic Scattering

The theory of Quantum ChromoDynamics is a broad subject for which there exist good reviews of theoretical[55], phenomenological[56], and experimental[57] natures. QCD is now as much a part of the paradigm for particle description as is the quark hypothesis. As such, it is important to seek clean tests of the theory -- tests which, if found not to stand the test of experiment, will cause us to re-evaluate the completeness of our understanding. Measurements which tell us more about the strong interaction and the nature of constituents are important, of course, but there is no substitute for tests which are unambiguously predicted before the experiment is done. Deep inelastic scattering offers a few possible tests of this kind.

Figure IV-1 illustrates the contributions to structure through leading order of the perturbative expansion. Figure IV-1a is the diagram contributing in a picture of "free quarks", and the zeroth approximation in a perturbative expansion. While this term is close enough to reality so that approximate scaling was recognized at low energies and corroborated at high energies, the contributions due to the strong interactions are eminently visible, as illustrated in the dependence on Q^2 at fixed x for the F_2 structure function in figure IV-2.[58]

Figure IV-1b and -1c illustrate leading order contributions.

Figure IV-1: Diagrams describing contributions from (a) free quarks; (b) gluon brehmstrahlung; and (c) gluon pair production to the deep-inelastic process.

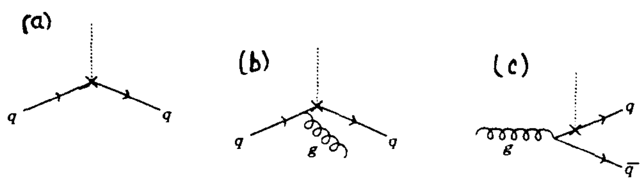

The first, denoted a flavor non-singlet contribution, arises due to the initial quark radiating a gluon just prior to the interaction. The second, in figure IV-1c, has an initial state gluon (flavor singlet) which produces a pair of quarks, one of which interacts with the virtual electroweak boson. Both of the latter diagrams are reduced relative to the first by one power in the quark-gluon coupling constant, α_s. This "constant" in fact depends on Q^2; in leading order

$$\alpha_s^{LO}(Q^2) = \frac{12\pi}{(33 - 2N_f)\ \ln(Q^2/\Lambda^2)} \qquad \text{(leading order)} \qquad \text{(IV-1)}$$

where N_f is the number of quark flavors contributing. For present deep-inelastic experiments, the energies dictate that $N_f = 4$.

Two points should be made about the discussion thus far. First, the discussion describes a perturbative expansion; it ignores many possible terms which are not part of this expansion. The latter are generally called "higher-twist" terms: instead of a logarithmic dependence on Q^2 as implied by the above equations, such terms would depend on a power of $1/Q^2$. One example of such a term would be the contribution to R from intrinsic transverse momentum of quarks inside the nucleon, as in equation III-1. Some effects due to the finite target mass of the nucleon can be described by Georgi-Politzer corrections.[59]

A second point is that we have illustrated the consequences of the perturbative expansion with the leading order diagrams and terms only. In fact, the analysis has been carried to next-to-leading order. There are several approaches; the most commonly used for comparison to experiment is a "minimum-subtraction" technique labelled $\overline{MS}$. The quark-gluon coupling parameter in next-to-leading order is

$$\alpha_s(Q^2) = \alpha_s^{LO}(Q^2)\left[1 - \frac{(102 - 38\, N_f/3)}{(11 - 2\, N_f/3)^2} \frac{\ln\,[\ln\,(Q^2/\Lambda_{\overline{MS}}^2)\,]}{\ln(Q^2/\Lambda_{\overline{MS}}^2)}\right] \qquad \text{(IV-2)}$$

in terms of the leading order parameter of equation IV-1. More detail on the next-to-leading order analysis is available.[60]

We return now to two specific predictions of perturbative QCD for deep inelastic scattering.

A. Prediction for R.

Recall the definition of R from equation I-10:

$$\frac{2xF_1}{F_2} = \frac{1 + 4M^2x^2/Q^2}{1 + R} .$$

The leading order QCD-prediction from the diagrams of figure IV-1 is

$$R(x,Q^2) = \frac{\alpha_s(Q^2)}{2\pi}\, x^2 \int_x^1 \frac{dz}{z^3} \left[\frac{8}{3} F_2(z,Q^2) + 4f(1 - \frac{x}{z})zG(z,Q^2)\right] \Big/ 2xF_1 \qquad \text{(IV-3)}$$

where $f = N_f$ (the number of flavors) in the neutrino case, and
$= \Sigma e_i^2$ (the sum over quark charges) for muon/electron scattering. (This assures that the same physical value of R results for both cases. Recall that the structure function, F_2, differs in the two cases by the quark charge squared.) The two terms on the right-hand side of this equation come from the two diagrams of the figure IV-1b and -1c, respectively. The integration over F_2 gives the contributions to non-colinearity that result from quark emission of a gluon prior to interaction; the integration over the gluon distribution $G(x,Q^2)$ gives the contribution from pair production of a quark-antiquark pair, one of which interacts with the propagator boson.

It should be noted that there will, in general, be additional contributions from target mass effects, intrinsic transverse momenta of the interacting quarks (as in equation III-11), etc. The target mass effects can be explicitly calculated.[61] Figure IV-2 shows recent data taken at SLAC to measure R in the low Q^2 region. The lower dotted curves give the QCD prescriptions (equation IV-3). The dashed curves give the predictions taking into account target mass effects. The QCD curves do not agree with the data in this low Q^2 regime. Even including the target mass effects (dashed curves) does not reproduce the data well in the low x, low Q^2 region. The continuous curves represent fits to the data using the QCD prediction with an adjustable non-perturbative term.

Figure IV-2: SLAC Measurements of R (symbols). See text for description of curves.

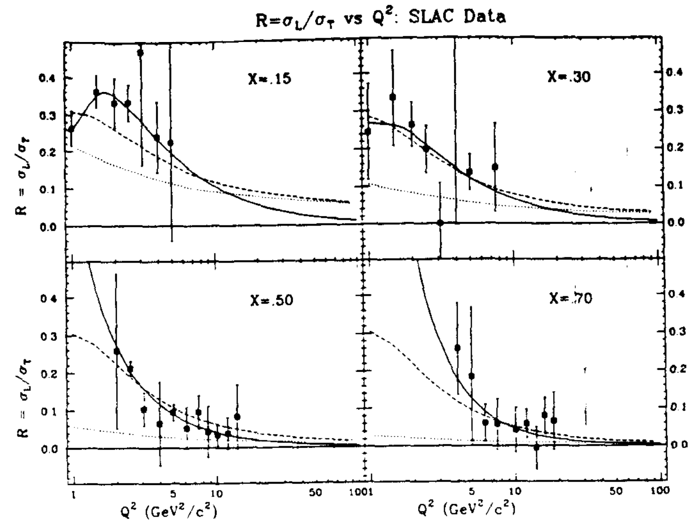

There are several measurements at higher energies which are consistent with the prediction of equation IV-3.[62] While consistent with the perturbative QCD-inspired prediction, these measurements do not demonstrate its validity. Taking a devil's advocate approach, the low energy data were parametrized as due solely to higher twist terms of the form $\alpha(x)/Q^2 + \beta(x)/Q^4$, in which the coefficients α and β were all less than or of order 1 GeV^n and the fit was quite acceptable. When this fit was compared to data taken at higher energies, the resulting agreement was not very different than the agreement with the QCD prediction.[63] We conclude that, while all existing data are consistent, this important test of perturbative QCD is not yet demonstrated experimentally.

B. Structure Function Evolution

The general scale-breaking features of deep inelastic structure functions are

(a) the dependence on Q^2 at fixed x is nearly logarithmic;

(b) the logarithmic slopes at small x are positive;

(c) the logarithmic slopes at large x are negative.

1. Singlet Structure Functions

This scale-breaking pattern of structure functions is beautifully described by perturbative QCD. Most structure functions, like F_2, are singlet structure functions. Their evolution is described[64] in perturbative QCD by

$$\frac{d\, F^S(x,Q^2)}{d\, \ln(Q^2)} = \frac{\alpha_s(Q^2)}{2\pi} \int_x^1 \left[F^S(z,Q^2)\, P_{qq}\left(\frac{x}{z}\right) + G(z,Q^2)\, P_{qG}\left(\frac{x}{z}\right) \right] dz\ . \qquad \text{(IV-4)}$$

The singlet function evolution requires both diagrams (b) and (c) of figure IV-1: the first and second terms of equation (IV-4) are the contributions of those diagrams, respectively. Here, F^S describes the quark density for radiation of a gluon and G describes the gluon density for quark pair creation. The "splitting functions" P_{qq} and P_{qG} are specified by QCD. Strictly, this equation is valid only in leading order, though if one allowed the predicted splitting functions to also depend on α_s then the equation would be valid in all orders.[65] Note that there is a completely analogous equation defining the evolution of the gluon distribution:

$$\frac{d\, G(x,Q^2)}{d\, \ln(Q^2)} = \frac{\alpha_s(Q^2)}{2\pi} \int_x^1 \left[F^S(z,Q^2)\, P_{Gq}\left(\frac{x}{z}\right) + G(z,Q^2)\, P_{GG}\left(\frac{x}{z}\right) \right] dz\ . \qquad \text{(IV-5)}$$

With these equations, and singlet data defining the structure function and its logarithmic derivatives, it is possible to extract values for the quark-gluon coupling, α_s, as well as the gluon distribution. We shall return to this point later.

2. Nonsinglet Evolution ... A Test of Perturbative QCD

For cases like xF_3, where only diagram (b) of figure IV-1 is relevant, the evolution is predicted to have a particularly simple form:

$$\frac{d\, F^{NS}(x,Q^2)}{d\, \ln(Q^2)} = \frac{\alpha_s(Q^2)}{2\pi} \int_x^1 F^{NS}(z,Q^2)\, P_{qq}\left(\frac{x}{z}\right) dz\ . \qquad \text{(IV-6)}$$

Physically, this simple description results from the fact that contributions from gluons are subtracted away in forming the structure function. For this case, the predicted logarithmic slope on the left-hand-side depends only on

a) parameters or functions (like P_{qq}) of the theory;

b) measured data, like $xF_3(x,Q^2)$;

c) the quark gluon coupling, α_s, which in a given order of perturbation theory depends on the single parameter, Λ or $\Lambda_{\overline{MS}}$.

Examination of the splitting function on the right hand side of equation IV-6 reveals that integral is positive for small x and negative for large x. Hence, the prediction for the nonsinglet logarithmic slope is that the slope goes through zero at an x that is independent of α_s. This behavior is qualitatively preserved in higher order. The consistency of the logarithmic slopes for nonsinglet structure functions at small and intermediate x-values constitutes a well-posed test for perturbative QCD.

Data have not, until now, corroborated this issue well. Figure IV-3 shows the data on logarithmic slopes from CDHSW,[66] along with predictions for various values of $\Lambda_{\overline{MS}}$. The data do not support the predictions. The authors, however, point out that this could be a consequence of correlated systematic errors of measurement rather than a failure of QCD. Neutrino data from the CCFR narrow band experiments[67] were statistically inadequate to answer this question definitively.

Figure IV-3: Logarithmic derivatives as a function of x. Slopes for $Q^2>2$ (circles); and $Q^2>5$ GeV^2 (squares).

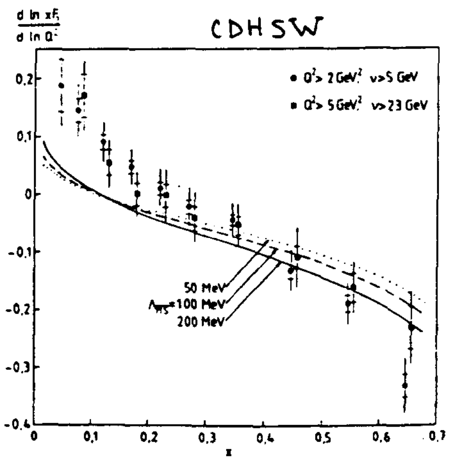

Figure IV-4 shows data on the logarithmic slopes of xF_3 from the newer wide band neutrino experiments of CCFR.[68] These data are consistent with the predictions of perturbative QCD, showing the expected behavior at small and intermediate values of x. We return to discuss this later.

Figure IV-4: The CCFR non-singlet slopes with the QCD prediction.

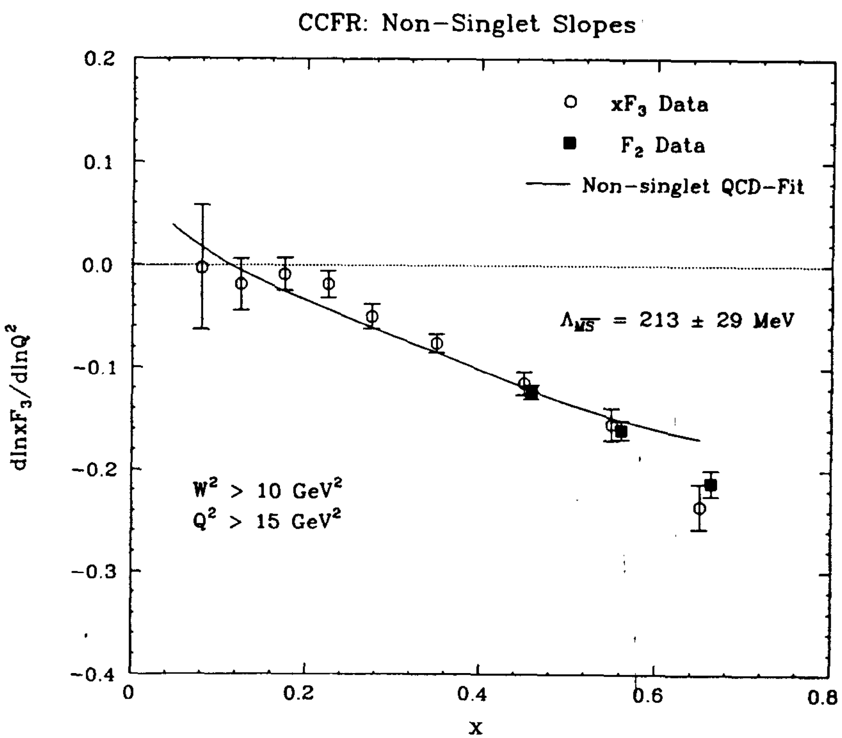

3. Singlet Evolution Revisited

Singlet structure functions (i.e., F_2) can be measured with both neutrino/antineutrino experiments and with muon/electron experiments. Historically, published data were fit to equations (IV-4,5) and parameters for $\Lambda_{\overline{MS}}$ and the gluon distribution, G(x), were extracted. The difficulty with these early fits was that, just as for the nonsinglet (neutrino) data just mentioned, the data from the CDHSW(ν)[69] and EMC(μ)[70] did not fit the hypotheses of QCD very well, as seen in figure IV-5.

The BCDMS collaboration published muon data on F_2 beginning in 1987 which fit the hypotheses for singlet evolution well.[71] They also approached the problem by dividing the regions between those at large and small x.

Figure IV-5: Singlet slopes and QCD fits (as analyzed by BCDMS) for (a) EMC and (b) CDHSW data.

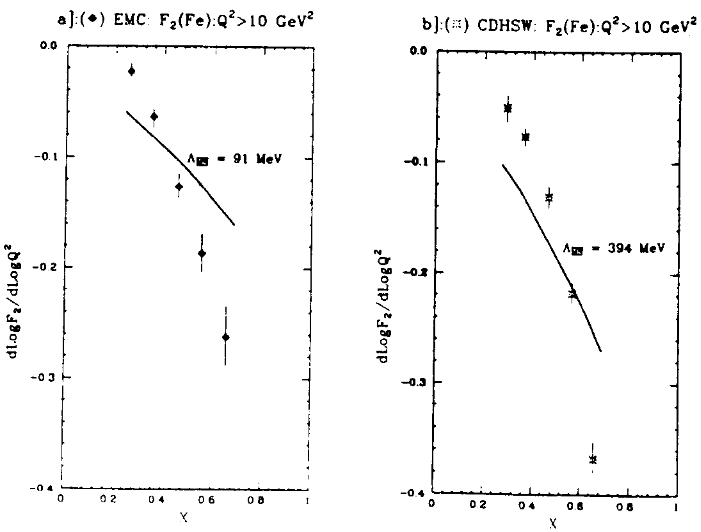

At large x, F_2 should become simple. We expect that in this region:

a) $R \to 0$;

b) $\bar{q} \to 0$;

c) $G \to 0$.

Under these circumstances, F_2 is essentially equal to xF_3, so that we are dealing with the nonsinglet evolution equation IV-6. In this region, one can extract the value of $\Lambda_{\overline{MS}}$.

The BCDMS group assumed that F_2 evolves like xF_3 for $x > .25$, and proceeded to fit to equation IV-6. They obtained good fits with consistent measures of $\Lambda_{\overline{MS}}$ for several different targets, including H_2, D_2, and C. Though their result was very sensitive to the overall calibration of the muon energy (at the level of 2×10^{-3}), they utilized the data to finalize this calibration by allowing it to vary within their direct error of measurement. Once a consistent fit was obtained at higher x, they utilized (in the case of H_2 and D_2) data at smaller values of x to extract the gluon distribution, as shown in figure IV-6.

Figure IV-6: The BCDMS measurements of the logarithmic slopes of F_2 for H_2 target data, with QCD fit.

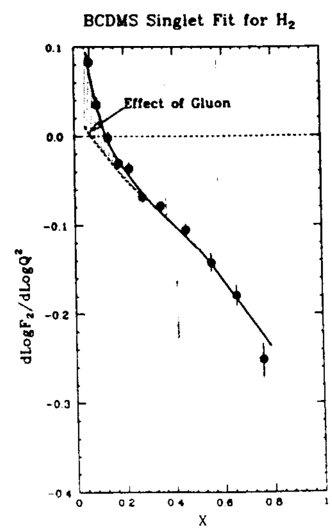

This was the first clean high-statistics demonstration of structure function consistency with the requirements of perturbative QCD. The extracted values of $\Lambda_{\overline{MS}}$ are trustworthy in that the parameters are extracted from data consistent with the theory in which $\Lambda_{\overline{MS}}$ originates. One concern about the gluon fits, however, is the need *to assume the absence of gluons and antiquarks for x > .25.* While they later iterate to show that this assumption is consistent with the data, this demonstration could be self-fulfilling.

New neutrino data on F_2 and xF_3, with high statistics and precision control over systematics, address this issue. As already discussed, the data of figure IV-4 show good agreement with the predictions for nonsinglet structure functions. The Q^2 dependence for F_2 is in good accord with expectations. Substitution of F_2 for xF_3 results in smaller statistical error. It is found, however, that the *antiquark component* $[x\bar{q}(x)/xF_3(x)]$ begins to be visible in F_2 for $x < .5$, as shown in table IV-1. The NLO values of $\Lambda_{\overline{MS}}$ are shown in the last column.

Table IV-1: $\bar{q}$-fraction at large x; effect on QCD fit (CCFR data).

x-bin	Antiquark Comp	NLO Lambda
no substitution		179 ± 36 MeV
0.65	-0.3 ± 0.7 %	220 ± 34 MeV
0.55	1.2 ± 1.0 %	213 ± 29 MeV
0.45	3.0 ± 0.7 %	215 ± 25 MeV

Hence, the substitution $F_2 \to xF_3$ for $x > .5$ is applied to obtain

$$\Lambda_{\overline{MS}} = 213 \pm 29 \pm 41 \text{ MeV}.$$

These results will be discussed next week at the topical conference by Sanjib Mishra.[72]

Table IV-2 shows a 1988 survey on measurements of the parameter, $\Lambda_{\overline{MS}}$, governing the quark-gluon coupling. It should be noted that until the measurements of 1987-88 by BCDMS, these data were not demonstrated to be in good accord with the theory. I have added at the bottom some more recent analyses.

Table IV-2: Older and more recent analyses for $\Lambda_{\overline{MS}}$.

Group	Year	Λ (MeV) in NLO	Data
CDHSW (WB)	1983	200 ± 100	xF_3, F_2
CHARM (WB)	1984	310 ± 140 ± 70	xF_3, F_2
EMC - H_2	1985	$105^{+55\,+85}_{-45\,-45}$	F_2 x > .35
EMC - D_2	1987	$65^{+95\,+155}_{-50\,-45}$	F_2 x > .35
CCFR (NB)	1987	$251^{+134}_{-115} \pm 89$	xF_3
BCDMS - C	1987	230 ± 20 ± 60	F_2 x > .275
BCDMS - H_2	1988	200 ± 22 ± 60	F_2 x > .275
BCDMS/SLAC-H_2	1990	250 ± 40	F_2 x > .275
BCDMS/SLAC-D_2	1990	260 ± 40	F_2 x > .275
EMC(reana)-H_2	1991	$211^{+82\,+84}_{-73\,-77}$	F_2 x > .275
CCFR (WB)	1991	213 ± 29 ± 41	xF_3, F_2 x > .5

V. Sum Rules

The Standard Model dictates that structure functions obey certain well-defined and measurable Sum Rules. These are in general motivated and predictable from the Operator Product Expansion and light-cone algebra. Sid Drell[73] has explained the origin and the fundamental aspects of the various sum rules from this point-of-view. Here, I would like take a more phenomenological perspective to describe how sum rules follow simply from the quark model, and how experiments compare to the predictions.

For pedagogical reasons, we ignore quarks more massive than u- and d-quarks, though their effects typically cancel anyway. (The strange quark density will be relevant and discussed in section D.) As defined in chapter III, the $u_p(x)$ and $d_p(x)$ distributions describe the frequency for finding u- and d-quarks, respectively, in the proton. The trick with the sum rules is to find simple relationships among the integrated totals:

$$U_p = \int u_p(x)dx \qquad \bar{U}_p = \int \bar{u}_p(x)dx \tag{V-1}$$

where the integration is understood to be over the entire domain of x. As stated previously, we expect from invariance under isospin (or SU_2) that the densities of u-quark in proton and d-quark in the neutron will be the same. It is absolutely clear from the baryon and isosopin assignment of quantum numbers that the integrated totals are the same:

$$U = U_p = D_n \qquad \bar{U} = \bar{U}_p = \bar{D}_n$$

and

$$D = D_p = U_n \qquad \bar{D} = \bar{D}_p = \bar{U}_n \tag{V-2}$$

The experimental difficulty with measuring sum rules comes about because the sums (or integrals) result by taking <u>differences</u> of structure functions or of cross-sections, <u>dividing</u> by x, and integrating. This weights small x data heavily: good resolution in this region is necessary. Also, it is very important that the coefficient of 1/x in the integrand approach zero as $x \to 0$. (Otherwise, the integral diverges.) This puts additional heavy emphasis on good relative normalization between the subtracted quantities.

A. Adler Sum Rule[74]

This relation, as mentioned by Drell, may be exact. It has been shown that there are no QCD corrections.[75] It comes from an integration over the F_2 structure functions obtained from neutrino-neutron and neutrino-proton scattering:

$$S_A = \frac{1}{2}\int_0^1 \frac{dx}{x}\left[F_2^{\nu n} - F_2^{\nu p}\right] . \tag{V-3}$$

From the quark-model representations of these, we obtain

$$\begin{aligned} S_A &= \int dx\ [d_n(x) + \bar{u}_n(x) - d_p(x) - \bar{u}_p(x)] \\ &= D_n + \bar{U}_n - D_p - \bar{U}_p \\ &= (U - \bar{U}) - (D - \bar{D}). \end{aligned} \tag{V-4}$$

Hence, the prediction is

$$S_A = 1 \qquad \text{(prediction)}. \tag{V-5}$$

Equation V-3 illustrates the need to obtain precise data at small x and for good relative normalization between data taken with neutrons (deuterium) and that taken with protons. The Adler sum rule is especially difficult because, as we have seen chapter III, the statistical accuracy of neutrino data with hydrogen and deuterium targets is not high. Nevertheless, there is one measurement in the literature:

$$S_A^{exp} = 1.01 \pm .20 \qquad \text{(V-6)}$$

and the Q^2-dependence is shown in figure V-1.[76] At the twenty percent level, the Adler sum rule is experimentally verified.

Figure V-1: The Q^2-dependence of the Adler sum rule measurement.

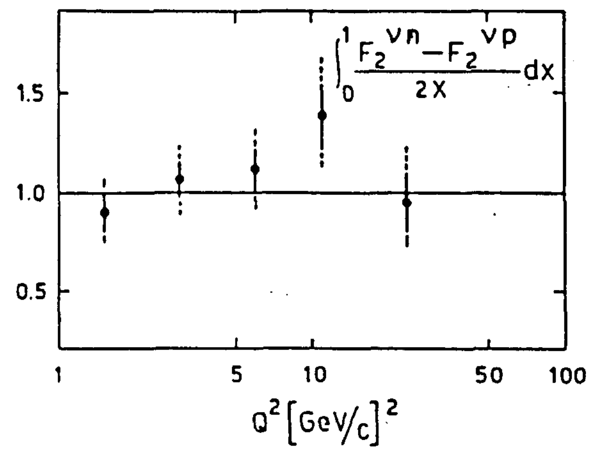

B. Gross - Llewellyn Smith (GLS) Sum Rule[77]

This prediction comes from the non-singlet neutrino structure function, $xF_3(x)$, obtained by subtraction of anti-neutrino from neutrino cross-sections on isoscalar (typically heavy nuclear) targets. It states

$$S_{GLS} = \int_0^1 \frac{xF_3^{\nu N}}{x} dx = (U - \bar{U}) + (D - \bar{D}) = 3. \qquad \text{(V-7)}$$

More precisely, it arises as the coefficient of $[1-(1-y)^2]$ in

$$(D_p+D_n-\bar{D}_p-\bar{D}_n) - (U_p+U_n-\bar{U}_p-\bar{U}_n)(1-y)^2. \qquad \text{(V-8)}$$

There are calculable QCD corrections to this sum rule.[78] In next-to-leading order,[79]

$$S_{GLS} = 3\ [1 - .48/\ln(Q^2/\Lambda^2)] \quad \text{predicted.} \qquad \text{(V-9)}$$

Because the nonsinglet structure function can be measured with a nuclear target, high statistical precision is attainable. The recent CCFR measurement is shown in figure V-2, in which the x-distribution of xF_3 and the integral above a given x are superimposed. This most precise measurement gives:[80]

$$S_{GLS} = 2.50 \pm .018 \pm .078\ . \qquad \text{(V-10)}$$

Figure V-2: The CCFR measurement of the Gross-LLewellyn Smith Sum Rule.

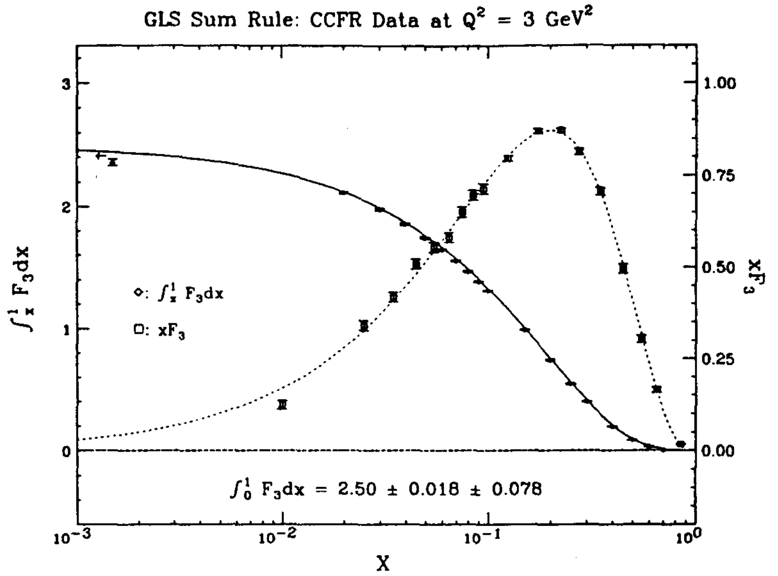

This can be compared to the expected value at $Q^2 = 3$ GeV^2 with $\Lambda_{\overline{MS}} = 213 \pm 50$ MeV:

$$S_{GLS} = 2.65 \pm .04 \quad \text{predicted.} \tag{V-11}$$

This 1.7 standard deviation difference is not in the best agreement. It should be noted that there could be limitations due to higher twist effects or scale uncertainty.[81] The measurements of this important sum rule over time is shown in figure V-3. Clearly even better precision is possible.

Figure V-3: The status of measurements for the Gross-LLewellyn Smith Sum Rule over time.

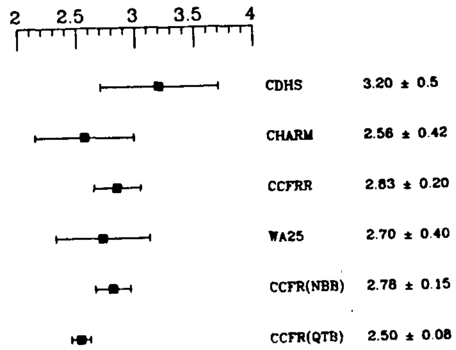

C. Gottfried Sum Rule[82]

This sum rule is measured with muon beams incident on hydrogen and deuterium targets. The definition is

$$S_G = \int_0^1 \frac{dx}{x}\left[F_2^{\mu n} - F_2^{\mu p}\right] \tag{V-12}$$

$$= [4(U_p+\bar{U}_p) + (D_p+\bar{D}_p) - 4(U_n+\bar{U}_n) - (D_n+\bar{D}_n)]/9$$

$$= [(U + \bar{U}) - (D + \bar{D})]/3 \,.$$

If one naively assumes[83] that the sea of u- and d- quarks and antiquarks are equal, then the prediction is

$$S_G = 1/3 \quad \text{for } \bar{U} = \bar{D}. \tag{V-13}$$

There are expected to be only very small QCD corrections to this sum rule.[84]

Until recently, the difficulty with obtaining high precision at low x has prevented this sum rule from being measured with high accuracy. There had been measurements by SLAC,[85] and by EMC,[86], and by BCDMS[87]. All had poor precision in the critical small x-region; the tendency in these experiments was to get a result lower than the prediction. The NMC experiment was designed for precision comparisons between different targets. They have made a good measurement of F_2^n/F_2^p to very small values of x.[88] Then, using the relation

$$F_2^p - F_2^n = 2\, F_2^d \frac{1 - F_2^n/F_2^p}{1 + F_2^n/F_2^p} \qquad \text{(V-14)}$$

and the world-averaged measurement of the F_2^d structure function, they obtain the data shown in figure V-4. Over their region of measurement:

$$S_G = .227 \pm .007 \pm .014 \quad \text{for} \quad .004 \le x \le .8\,. \qquad \text{(V-15)}$$

Figure V-4: The NMC measurement of $F_2^p(x)-F_2^n(x)$ and the Gottfried Sum Rule. The circle and trigangles are the integrals from two different methods.

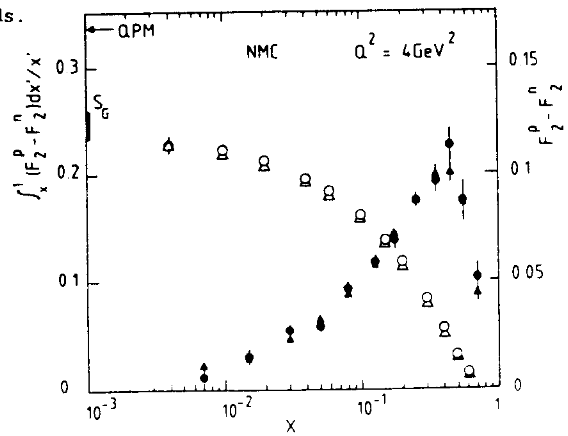

The small x data, like those for the GLS sum rule, are consistent with a power law dependence on x. Extrapolation to the region below x = .004 gives

$$S_G = .240 \pm .016 \qquad 0 < x < 1. \qquad \text{(V-16)}$$

This value is more than five standard deviations from the predicted value of .33 above. This has been viewed by some as a serious problem, perhaps in extrapolating to small x.[89] But is it a problem or does it simply reflect an interesting property of the nucleon?[90]

Note that with isospin symmetry, the prediction (V-12) for the Gottfried Sum Rule is

$$S_G = [(U-\bar{U}) + (D-\bar{D})]/3 + 2(\bar{U}-\bar{D})/3. \qquad \text{(V-17)}$$

The first term is just the sum of the net number of u- and d-quarks in the proton so

$$S_G = 1/3 \;+\; 2(\bar{U}-\bar{D})/3. \qquad \text{(V-18)}$$

But there is no a priori reason why the numbers of $\bar{u}$- and $\bar{d}$-quarks must be equal! That is, $\bar{U} \neq \bar{D}$ does not violate any basic principle. Note that this is the first sum rule in which the quantum numbers contributed by constituent quarks has not been subtracted, flavor-for-flavor, to arrive at only net nucleon quantum numbers.

Physically, the implications of $\bar{U} < \bar{D}$ are not even particularly unexpected. It simply means that gluon pair creation of $(u,\bar{u})$ occurs less often that pair creation of $(d,\bar{d})$ in the proton. But, the number of u- quarks is larger than d-quarks in the proton, and this has implications for the x-dependence of the valence quark densities on x. (Recall that the d-quark distribution falls faster than the u-quark distribution by approximately one power of [1-x]. See chapter III.) Is it so unreasonable, since the gluon contribution to u- and d- quarks at lower x occurs as pairs of quark-antiquark, that more acceptable wavefunctions for the Pauli principle will occur with differing numbers of u- and d-quarks in the ocean? There may, of course, be other reasons for antiquark asymmetries, like a different mass for the u- and d-quarks. It is interesting that this "problem" was anticipated more than a decade ago by Field and Feynman,[91] when they were putting together the earliest attempt at parametrizations of quark densities. The data even then suggested such an effect, and they had no compunctions about assuming differing numbers of u- and d-quarks in the sea.

What must be true is that the number of these quarks in the ocean as $x \to 0$ must be equal; otherwise, sum rules will not even converge. If one parametrizes the dependences of the sea quarks as

$$x\bar{u}(x) = c\,(1-x)^{\eta}$$
$$x\bar{d}(x) = c\,(1-x)^{\lambda} \qquad \text{(V-19)}$$

then, Field and Feynman found that $\eta - \lambda \simeq 3$, to best fit available data. For the present data, the difference in the exponents must be even greater.[92]

D. The Bjorken Sum Rule[93]

Here is a sum rule which has variously been described as "worthless" by Bjorken in 1966 to "absolutely essential if QCD is correct" by Bjorken in 1990.[94] The latter quote represents a general consensus about the importance of this relation today. To measure and verify the rule requires polarized electrons, polarized protons, and polarized neutrons. It is obviously not easy to do! For a detailed explanation of both experimental and theoretical aspects of this important problem, there is an excellent review.[95] An abbreviated explanation follows.

If one scatters polarized electrons from a polarized proton target, the difference in the differential cross-sections for proton polarization parallel to and antiparallel to the beam polarization is given by

$$\frac{d^2[\sigma(\uparrow\uparrow)-\sigma(\uparrow\downarrow)]}{dx\,dy} \xrightarrow[x \text{ fixed}]{\nu\to\infty} \frac{e^4}{2\pi\,Q^2}\left[1-\frac{y}{2}\right] g_1{}^p(x) \qquad \text{(V-20)}$$

$$\text{where } g_1{}^p(x) = \Sigma\, e_i{}^2\,[\rho_i{}^{\uparrow}(x) - \rho_i{}^{\downarrow}(x)].$$

Here the sum extends over all quark types inside the proton, with weighting by square of the quark charges (e_i, in units of the electron charge) and the difference between the quark density (ρ) with quark spin along and opposite, respectively, to that of the incident electron.

It clearly follows that the asymmetry is

$$A = \frac{d^2[\sigma(\uparrow\uparrow)-\sigma(\uparrow\downarrow)]}{d^2[\sigma(\uparrow\uparrow)+\sigma(\uparrow\downarrow)]} \simeq \frac{g_1(x)}{F_1(x)} . \qquad \text{(V-21)}$$

Hence, measurement of the asymmetry for proton and neutron targets permits measurement of the "spin structure functions," $g_1{}^p$ and $g_1{}^n$, respectively.

The Bjorken Sum Rule relates the integrals for the proton and neutron spin structure functions:

$$S_{BJ} = \int_0^1 [g_1{}^n(x) - g_1{}^p(x)]dx = \frac{1}{2}\,(e_u{}^2 - e_d{}^2)[(U^{\uparrow}-U^{\downarrow})-(D^{\uparrow}-D^{\downarrow})] \qquad \text{(V-22)}$$

where the quark charges are shown explicitly, and for example

$U^{\uparrow} - U^{\downarrow} = \Delta U$ is the net number of u-quarks with spin aligned.

Since the quantity in brackets is just the expectation of the Pauli spin-matrix:

$$(U^{\uparrow} - U^{\downarrow}) - (D^{\uparrow} - D^{\downarrow}) = \langle\sigma_z\rangle = |g_A/g_V|$$

or the ratio of the axial vector to vector β-decay weak coupling constants. We therefore obtain

$$S_{BJ} = \frac{1}{6}\left|\frac{g_A}{g_V}\right|\left[1 - \frac{\alpha_s}{\pi}\right] . \qquad \text{(V-23)}$$

The last term is the first-order QCD correction.[96]

The terms on the right-hand side are reasonably well known. One obtains for $|g_A/g_V| = 1.254 \pm .006$ and $\alpha_s = .27 \pm .02$ (at $Q^2 = 10.7$ GeV^2)

$$S_{BJ} = .191 \pm .002 \quad \text{predicted.} \qquad \text{(V-24)}$$

Figure V-5: The EMC measurement of $g_1{}^P(x)$.

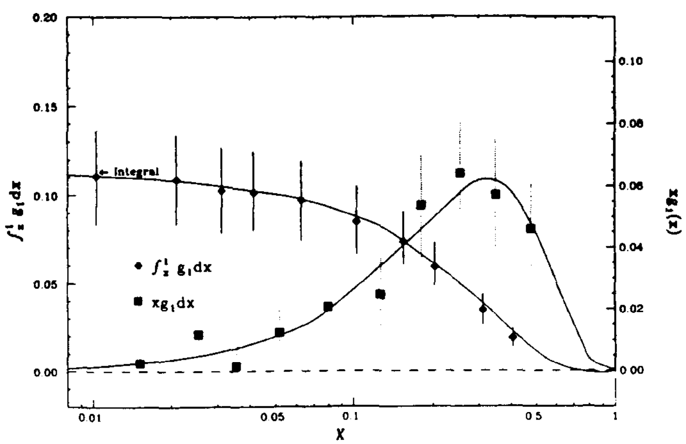

This sum rule is untested as yet. It awaits a good measure of the spin structure function for the neutron, $g_1{}^n$. There does exist, however, good data on the proton spin structure function from the EMC collaboration, as shown in figure V-5.[97] The result is

$$\int g_1{}^P(x)\ dx = 0.114 \pm .012 \pm .026 \quad \text{at } Q^2 = 10.7\ GeV^2. \qquad \text{(V-25)}$$

While we cannot yet test the Bjorken Sum Rule, there are some interesting implications for this result. There is a sum rule,[98] relying on flavor SU_6, which predicts the integral for the proton spin structure function if the effects of asymmetry due to strange quarks may be ignored. This predicts

$$\int g_1{}^P(x)\ dx = .189 \pm .005 \qquad \text{(V-26)}$$

which is about 2.5 standard deviations from the measured value.

But even without the Ellis-Jaffe Sum Rule, there are some perplexing aspects to the measurements if one ignores the strange quarks. From the definition above (V-20) of the spin structure functions, the contributions to the integrals from the u- and d-quarks are calculated and shown in table V-1 below. The only assumption here is that the strange quarks are unimportant. The evaluation of the neutron integral comes from <u>assuming</u> the validity of the Bjorken Sum Rule and using the measurement (V-26).

Table V-1: Evaluations of Contributions to proton spin from EMC data.

Integral	Quark Asymmetry	Value	from
$\int g_1^p(x)\,dx$	$\frac{1}{2}\left[\frac{4}{9}\Delta U + \frac{1}{9}\Delta D\right]$	.114 ± .030	experiment
$\int g_1^n(x)\,dx$	$\frac{1}{2}\left[\frac{1}{9}\Delta U + \frac{4}{9}\Delta D\right]$	-.077 ± .030	assume BJ sum rule
SUM	$\frac{5}{18}\left[\Delta U + \Delta D\right]$	.037 ± .060	sum

The implication is that the contribution of u- and d-quarks to the proton spin is

$$\Delta U + \Delta D = (.037)(18/5)$$

$$= .14 \pm .09 \pm .19 \,. \qquad \text{(V-27)}$$

That is, the valence quarks of the proton carry only about 14% (to about a factor two precision) of the proton spin. This conclusion persists even if one drops the assumption about the strange quarks. If, in addition to the Bjorken Sum Rule and the EMC measurement of $\int g_1^p(x)\,dx$, one assumes the validity of the Ellis-Jaffe Sum Rule, then the <u>three</u> unknowns (ΔU, ΔD, and ΔS) may be determined. This has been done[99] and one still obtain the contributions from these to be about 12% with similar errors to those above.

It does seem perplexing that, when the constituent quark model does so well in explaining the regularity of nucleon properties, one finds that the quarks which define the proton quantum numbers have so little to do with its net spin. There are many explanations for why this should happen. Some would have the gluons carrying the bulk of the nucleon spin,[100] while others would have the average quark spin and gluon spin small with the bulk of the proton spin being principally a consequence of orbital angular momentum.[101]

The measurement of the proton spin structure function has revitalized an interest in polarization and spin effects generally. It leads us to believe that a test of the fundamental Bjorken Sum Rule could be made, and may lead us to measurements which will tell us more about nucleon spin structure generally.

VI. Anomalies in Deep Inelastic Scattering

In this short time, it is impossible to do justice to all the various searches for anomalies that have taken place using the deep inelastic process as a tool to discover new processes. In one case that we have seen, neutral currents, deep inelastic scattering was critical both for finding the phenomenon, corroborating it, and for demonstrating its properties.

Beyond this, there have been searches for massive leptons of various kinds, in the early days for isotriplet charged and associated neutral partners of existing leptons, motivated by gauge theories;[102] and more recently, for neutral leptons motivated by grand unified and left-right symmetric models.[103] These have set interesting limits, but to date have not established the existence of such particles. Deep inelastic scattering has been an important tool for seeking evidence for oscillation of neutrinos into other flavors: no positive evidence has been forthcoming thus far on this issue.[104] There was an incipient anomaly for awhile in the production of same-sign muons by neutrinos,[105] but this has been set to rest[106] in 1988 by doing the experiment at twice the energy. There are clearly many ways that deep inelastic scattering experiments, both of fixed-target type and of the colliding beam (HERA) type, can seek out anomalous phenomena. Experimenters will clearly keep trying.

VII. Conclusion

The great discovery of scaling has led us into more than two decades of unique and exciting measurements. The discovery was great because it changed the way we think about the physical world in a very fundamental way. The measurements since then have corroborated this picture, and expanded our knowledge of the details.

The "new" field, Deep Inelastic Scattering, still goes strong. Much remains to be done at all energies.

I would like to acknowledge my colleagues in the CCFR for useful and interesting discussions on some of the material here, particularly Sanjib Mishra, Arie Bodek, and Mike Shaevitz. Communications with other physicists, including Ian Hinchcliff, Tim Londergan, Chris Quigg and Steve Ritz were very useful. Finally, I would like to thank the organizers of this summer school for their generous hospitality during my stay, as well as for bringing some very stimulating people together. I learned as well as taught during this period.

REFERENCES:

1/ G. Miller, et al., Phys Rev D5,6528(1972);
A. Bodek, et al., Phys Rev Lett 30,1087(1973).

2/ J.D. Bjorken and E. Paschos, Phys Rev 185,1975(1969).

3/ R.P. Feynman, Phys Rev Lett 23,1415(1969);
R.P. Feynman, Photon-Hadron Interactions, Benjamin, 1972.

4/ T. Eichten, et al., Phys Lett 46B,274(1973).

5/ F. Sciulli, et al., "Neutrino Physics at Very High Energies", Fermilab Proposal E21 (1970), unpublished.

6/ M. Gell-Mann, Phys Lett 8,214(1964).

7/ S. Drell, lectures in this summer school (1991).

8/ C.G. Callan and D.J. Gross, Phys Rev Lett 22,156(1969).

9/ T. Eichten, et al, op cit.

10/ B. C. Barish, et al., Phys Rev Lett 35,1316(1975).

11/ B. C. Barish, et al., Phys Rev Lett 39,1595(1977);
P. C. Bosetti, et al., Phys Lett 70B,273(1977);
J.G.H. de Groot, et al., Z Phys C1,143(1979);
R. Blair, et al., Phys Rev Lett 51,343(1983).

12/ H. Abramowicz, et al., Z Phys C17,282(1983);
R. Blair, et al., Phys Rev Lett 51,343(1983);
F. Sciulli, "Lepton Hadron Reactions", Proceedings of the 1985 Intl Symposium on Lepton and Hadron Interactions at High Energies, Kyoto, p. 7.

13/ F. Sciulli, op cit (1985);

Continued from previous page

M. W. Krasny, et al., Proc. Int. Europhysics Conf on High Energy Physics, Bari (1985), p. 555.
J. P. Berge, et al., Z Phys C35,443(1987).

14/ Particle Data Group, Phys Lett 170B, 84(1086).

15/ S. Mishra, et al., CCFR topical conference talk at this summer school (1991).

16/ A. Benvenuti, et al., Phys Rev Lett 33,984(1974);
A. Benvenuti, et al., Phys Rev Lett 34,597(1975);
A. Benvenuti, et al., Phys Rev Lett 36,1478(1976).

17/ H.E. Fisk and F. Sciulli, Ann Rev Nucl Part Sci 32,499(1982) [review];
M. Holder, et al., Phys Rev Lett 39,433(1977);
B.C. Barish, et al., Phys Rev Lett 40,1414(1978);
J.G.H de Groot, et al., Z Phys C1,143(1979);
S.M. Heagy, et al., Phys Rev D23,1045(1981).

18/ P. Auchincloss, et al., Z Phys C48,411(1990).

19/ S. R. Mishra, et al., op cit (1991).

20/ K. Bazizi and S.J. Wimpenny, UC-Riverside preprint UCR-DIS-91-02 (July 1991).

21/ Weinberg, S. Phys. Rev. Lett. 19, 1264(1967).
Salam, A. Elementary Particle Theory: Relativistic Groups and Analyticity (Nobel Symposium No. 8), edited by N. Svartholm (Almqvist and Wiksell, Stockholm), p. 367 (1968).

22/ F. Sciulli, Progress in Part and Nucl Physics 2,41(1979).

23/ G. t'Hooft, Phys Lett 37B,195(1971);
M. Veltman, Proc 6th Intl Symp Electron and Photon Int at High Energies, Bonn (1973), p. 420, and references therein.

24/ See, eg, J.D. Bjorken, Proc of XVI Intl Conf on HEP, vol II, Batavia, IL (1972).

25/ D. Perkins, Proc of XVI Intl Conf on HEP, vol IV, Batavia, IL (1972).

26/ G. Myatt, Proc 6th Intl Symp Electron and Photon Int at High Energies, Bonn (1973), p. 389.

27/ F.J. Hasert, et al., Phys Lett 46B,138(1973).

28/ F.J. Hasert, et al., Phys Lett 46B,121(1973).

29/ D. Perkins, op cit.

30/ B. Aubert, et al., Phys Rev Lett 32, 800(1974);
B. Aubert, et al., Phys Rev Lett 32, 1454(1974);
B. Aubert, et al., Phys Rev Lett 32, 1457(1974).

31/ D.C. Cundy, Proc of XVII Intl Conf on HEP, Bonn, FRG (1974), p.IV-131 .

32/ J. Sacton, Proc of XVII Intl Conf on HEP, Bonn, FRG (1974), p. IV-121.

33/ W. Lee, Proc of XVII Intl Conf on HEP, Bonn, FRG (1974), p. IV-127.

34/ B.C. Barish, et al., Proc of XVII Intl Conf on HEP, Bonn, FRG (1974),
p. IV-111;
B.C. Barish, et al., Phys Rev Lett 34,538(1975).

35/ See, eg Particle Data Group, Phys Lett 239,III-56(1990).

36/ S.R. Mishra, et al., op cit (1991);

Continued from previous page
W.C. Leung, et al., submitted to Phys Rev Lett.
W.C. Leung, PhD Thesis Columbia University 1992.

37/ C. Peroni, et al., Proc of Workshop on Hadron Structure and Parton Distributions, Fermilab, April 1990, p. 41.
S. Aid, et al., Proc of Workshop on Hadron Structure and Parton Distributions, Fermilab, April 1990, p. 58.

38/ S.R. Mishra and F. Sciulli, Ann Rev of Nucl and Part Sci 39,259(1989).

39/ W.K. Tung, private communication.

40/ K. Bazizi and S.J. Wimpenny, op cit (July 1991).

41/ A. deRujula, et al., Rev Mod Phys 46,391(1974);
R.M. Barnett, Phys Rev Lett 36,1163(1976), Phys Rev D14,70(1976);
H. Georgi and H.D. Politzer, Phys Rev D14,1829(1976).

42/ H. Abramowicz, et al., Z Phys C15,19(1982);
B. Strongin, et al., Phys Rev D43,2778(1991);
C. Foudas, et al., Phys Rev Lett 64,1207(1990), and next reference.

43/ M.H. Shaevitz, Nucl Phys B19,270(1991).

44/ M.H. Shaevitz, op cit.

45/ P.N. Harriman, et al., Proc of Workshop on Hadron Structure and Parton Distributions, Fermilab, April 1990, p. 338.

46/ A.H. Mueller and J. Qiu, Nucl Phys B268,427(1986);
J. Qiu, Nucl Phys B291,46(1987);
E.L. Berger and J. Qiu, Phys Lett B206,141(1988).

47/ S. Aid, et al., S. Aid, et al., Proc of Workshop on Hadron Structure and Parton Distributions, Fermilab, April 1990, p. 58.

48/ L. Frankfurt and M. Strickman, Phys Rep 160,235(1987).

49/ A. Arneodo, et al., Nucl Phys B333,1(1990);
S. Aid, et al., op cit (1990).

50/ J.J. Aubert, et al., Phys Lett B123,275(1983).

51/ A. Bodek, et al., Phys Rev Lett 50,1431(1983); 51,534(1983).

52/ E.L. Berger and F. Coester, Annu Rev Nucl Part Sci 37,463(1987).

53/ R.P. Feynman, Photon Hadron Interactions, Benjamin, NY (1972);
F. Close, An Introduction to Quarks and Partons, Academic Press, NY (1979).

54/ S. Dasu, et al., Phys Rev Lett 60,1061(1988).

55/ F. Wilczek, Annu Rev Nucl Part Sci 32,177(1982).

56/ G. Altarelli, Annu Rev Nucl Part Sci 39, 357(1989).

57/ T. Hansl-Kozanecka, lectures at this summer school (1991).

58/ S.R. Mishra, et al., op cit (1991);
P.Z. Quintas, et al., submitted to Phys Rev Lett.

59/ H. Georgi and D. Politzer, Phys Rev D14,1829(1976).

60/ G. Altarelli, op cit (1989).

61/ S. Dasu, et al., Phys Rev Lett 61,1061(1988).

62/ J.J. Aubert, et al., Nucl Phys B272,158(1986);
A.C. Benvenuti, et al., Phys Lett B195, 91(1987);

Continued from previous page
P. Buchholz, in Proc Int Europhysics Conf on High Energy Physics, Bari (1986);
J.J. Aubert, et al., Nucl Phys B259,189(1985);
A. Benvenuti, et al., Phys Lett B223,485(1989);
A. Benvenuti, et al., Phys Lett B223,592(1989).

63/ S.R. Mishra and F. Sciulli, Phys Lett B244,341(1990).

64/ G. Altarelli and G. Parisi, Nucl Phys B126,298(1977).

65/ G. Altarelli, op cit (1989).

66/ P. Berge, et al., Z Phys C49,187(1991).

67/ E. Oltman, et al., to be published in Z Phys.

68/ S.R. Mishra, et al., op cit (1991);
P.Z. Quintas, et al., submitted to Phys Rev Lett (1992).

69/ P. Berger, et al.,op cit.

70/ J.J. Aubert, et al., Nucl Phys B272,158(1986).

71/ A.C. Benvenuti, et al., Phys Lett B195, 91(1987).
A.C. Benvenuti, et al., Phys Lett B195, 97(1987).

72/ S.R. Mishra, et al., op cit (1991); P. Quintas, et al, op cit (1992).

73/ S. Drell, op cit (1991).

74/ S.L. Adler, Phys Rev 143;1144(1966).

75/ W.A. Bardeen, et al., Phys Rev D18,3998(1978).

76/ D. Allasia, et al., Phys Lett B135,231(1984); Z Phys C28,321(1985).

77/ D.J. Gross and C.H. Llewellyn Smith, Nucl Phys B14,337(1969).

78/ M.A.B. Beg, Phys Rev D11,1165(1975).

79/ W.A. Bardeen, et al., op cit (1978).

80/ S. R. Mishra, et al., op cit (1991).
W. C. Leung, et al., submitted to Phys Rev Lett.

81/ T. Hansl-Kozanecka, op cit (1991).

82/ K. Gottfried, Phys Rev Lett 18,1154(1967).

83/ S.R. Mishra and F. Sciulli, op cit (1989).

84/ D.A. Ross and C.T. Sachrada, Nucl Phys B149,497(1979).

85/ A. Bodek, et al., Phys Rev Lett 30,1087(1973).

86/ J.J. Aubert, et al., Nucl Phys B293,(1987).

87/ A.C. Benvenuti, et al., Phys Lett 237B,592(1990);
A.C. Benvenuti, et al., Phys Lett 237B,599(1990).

88/ D. Allasia, et al., Phys Lett B249,366(1990);
P. Amaudruz, et al., Phys Rev Lett 66,2712(1991).

89/ See, for example, A.D. Martin, et al., Phys Lett B252,653(1990).

90/ E. Eichten, et al., Fermilab PUB 91/272(1991).

91/ R.D. Field and R.P. Feynman, Phys Rev D15,2590(1977).

92/ E.J. Eichten, et al., op cit.

93/ J.D. Bjorken, Phys Rev 148,1467(1966).

94/ C. Prescott, private communication (1991).

95/ V. Hughes and J. Kuti, Annu Rev Nucl Part Sci 33,611(1983).

96/ W.A. Bardeen, et al., op cit (1978).

97/ J. Ashman, et al., Phys Lett B206,364(1988).

98/ J. Ellis and R.L. Jaffe, Phys Rev D9,1444(1984).

99/ J.T. Londergan and S. Kumano, Proc of Telluride Conf on Spin and Isosopin, Telluride, CO (March 1991), U Indiana preprint IU/NTC 91-02.

100/ M. Anselmino and E. Leader, Preprint NSF-ITP-88-142 (1988);
M. Anselmino, et al., Preprint NSF-ITP-88-94 (1988);
A.V. Efremov and O.V. Teryaev, JINR Rep E2-88,287(1988);
G. Altarelli, et al., Phys Lett B212,391(1988);
R.D. Carlitz, et al., Phys Lett B214,229(1988).

101/ S. Brodsky, et al., Phys Lett 206B,309(1988);
J. Ellis, et al., Phys Lett 213,73(1988).

102/ B.C. Barish, et al., Phys Lett 32,1387(1974).

103/ S.R. Mishra, et al., Phys Rev Lett 59,1397(1987).

104/ See, for example, F. Vannucci, Proc of the 13th Intl Conf on Neutrino Physics and Astrophysics, Boston (1988), p. 46.

105/ M. Jonker, et al., Phys Lett B107,241(1981);
T. Trinko, et al., Phys Rev D23,1889(1981);
K. Nishikawa, et al., Phys Rev Lett 46,1555(1981); 541336(1985);
H. Burkhardt, et al., Z Phys C31,39(1986);
K. Lang, et al., Z Phys C33,483(1987).

106/ B. Schumm, et al., Phys Rev Lett 60,1618(1988).